Epigenetic Control of Functional Axon Regeneration

by
Jessica Bailey Walters Cassin

A dissertation submitted to Johns Hopkins University in conformity with the requirements of the degree of Doctor of Philosophy

Baltimore, Maryland
August 2017

ABSTRACT

The failure of central nervous system axons to regenerate is a known consequence of traumatic injury and neurodegenerative disease. The central nervous system's regenerative capacity starkly contrasts with the peripheral nervous system, which demonstrates robust regeneration following injury. This ability is due to factors both extrinsic and intrinsic to the cell. Extrinsically, the environment of the central nervous system is inhospitable, presenting both physical and chemical barriers to regeneration. However, extrinsic factors are not the only component. When placed in a peripheral nervous context, central nervous system neurons still show only modest gains in regeneration. Intrinsically, the peripheral nervous system is able to upregulate genes known as regeneration associated genes which are important for the system's ability to regenerate. These genes, when expressed in a central nervous system neuron can promote gains in regeneration, although not to the same extent as the peripheral nervous system.

Despite an identical genetic complement, the central nervous system is unable to independently mobilize regeneration associated genes and promote regeneration. For this reason, we hypothesized that epigenetic differences between the central and peripheral nervous systems may be responsible. These epigenetic signatures are acquired by cells as they mature and differentiate. DNA methylation and chromatin structure are positioned so as to protect cell identity and allow expression of genes necessary for that cell's function. Adult neurons must be tightly regulated. As such, many genes responsible for the growth and

regeneration abilities seen in embryonic neurons are epigenetically silenced once the cell is fully differentiated.

We show that Tet3, a DNA demethylase, is essential for regeneration in the PNS. In our model, Tet3 activates a suite of regeneration association genes necessary to initiate the regeneration program in the peripheral nervous system. Tet3 accomplishes this by selectively demethylating key regions of essential regeneration associated genes and allowing their expression. Without Tet3, the cell is unable to achieve functional regeneration.

This study highlights the precise and delicate nature of regeneration in the peripheral nervous system and underscores the need for a holistic approach to activating regeneration in the central nervous system. Future studies will need to further refine the role of these dual highly regulated processes, transcription and translation, to unlock the regenerative potential of the central nervous system.

Thesis Advisor: Dr. Hongjun Song

Thesis Reader: Dr. Guo-li Ming

PREFACE

Taking on a PhD is not a decision to be made lightly. Before starting my graduate work, I heard about the horror stories and the successes, the competition and the lifelong friendships. While I knew I was ready to embark on my PhD, if I'm honest, none of the descriptions truly prepared me for what the substance of being a graduate student really is. It is the best/worst time. It's long days, longer nights, and surprisingly short years. It's a marathon that often must be run like a sprint. There are hurdles and obstacles, experiments that fail for 15th time in a week, impossible deadlines, and missing out on a lot of fun adventures while you're, say, writing a dissertation. Thankfully though, it's not without its silver lining.

In my case, that silver lining is the cloud of people who have surrounded me throughout my PhD. Although I don't think that the black-and-white words of a page can adequately express my gratitude, I want to begin this dissertation by thanking the individuals who have offered so much love, support, and guidance over the past four years. The Human Genetics program and the Song-Ming lab have been instrumental in shaping me into the scientist that I am today. The coursework is tough, and the expectations are high, but both my lab and my program have provided me every opportunity to grow, learn, and succeed. I have grown immeasurably as a scientist and as a person through their support and effort. This project would not have been possible without my two co-authors, Yi-lan Weng and Ran An. The work contained here was a collaborative effort amongst the three of

us. I'm thankful they were willing to share their experience and their project with me.

I would also like to thank my friends, both from within the walls of Hopkins and those without. I do not think I could have successfully completed graduate school without them. They have brought meals and coffee and wine, edited papers, studied for exams, stayed with me though long days in the lab, and truly cared for me and my family though this whole process.

I have grown up as the granddaughter of coal miners and farmers, and yet, am finishing my PhD at Johns Hopkins. This is possible because my family has always made sure that I have had every opportunity for success imaginable, even when it meant a lot of sacrifice. I am so thankful for a family who encouraged my love of science. In particular, I'm thankful for my mother and father who made sure I had a secure, happy childhood that was full of imagination and fun. And even though I'm now miles away, they have continued to love and encourage me from afar.

Finally, I cannot begin to express the debt of gratitude that I owe to my husband. There are not words sufficient to explain his unending support for me. Rather than try to explain, I'll just close with: Thank you.

TABLE OF CONTENTS

LIST OF TABLES

CHAPTER 5

LIST OF FIGURES

CHAPTER 3

CHAPTER 4

CHAPTER 5

ABBREVIATIONS

5caC	5-carboxylcytosine
5fC	5-formylcytosine
5hmC	5-hydroxymethylcytosine
5mC	5-methylcytosine
AAV	adeno-associated virus
ChIP	chromatin immunoprecipitation
CNS	central nervous system
CpG	cytosine phosphate guanine
CRISPR	clustered regularly interspaced short palindromic repeats
ctrl-shRNA	control shRNA
D1	day 1
DE1	distal enhancer 1
DNMT	DNA methyltransferase
DRG	dorsal root ganglion
FACS	fluorescence-activated cell sorting
GADD45	growth arrest and DNA-damage-inducible protein 45
HAT	histone acetyltransferase
HDAC	histone deacetylase
HDM	histone demethylase
HMT	histone methyltransferase
IHC	immunohistochemical
KD	knockdown
KO	knockout
MSRE	methylation sensitive restriction enzymes
m^6A	N6-methyladenosine
m^1A	N1-methyladenosine
m^5C	5-methylcytosine
mTOR	mammalian/mechanistic target of rapamycin
PNS	peripheral nervous system
RAG	regeneration associated gene
shRNA	small hairpin RNA
SNL	sciatic nerve lesion
TET	ten-eleven translocation
TDG	thymine DNA glycosylase
WT	wildtype

CHAPTER 1 - INTRODUCTION

1.1 Nervous system injury and disease

The central nervous system (CNS), composed of the brain, optic nerve, and spinal cord, is unable to regenerate. This failure contributes greatly to CNS morbidity and mortality. When insult occurs to a CNS neuron, such as in the case of stroke, injury, or neurodegenerative disease, the system is unable to repair the damage and the neuron dies [1]. Because the CNS is largely composed of post-mitotic neurons without a stem cell reservoir, lost neurons cannot be replaced. Thus, injury and disease lead to loss of normal CNS function [2]. In stark contrast, the peripheral nervous system (PNS) has robust, sustained regeneration. Although many inherent differences exist between the CNS and the PNS, much can be gained from a deeper understanding of the PNS's regenerative program.

1.2 Wallerian degeneration

Soon after axonal injury, in both the CNS and PNS, Wallerian degeneration (WD) is activated [3]. In this process, the molecular components of injured axons are systematically disassembled and myelin is broken down, generating debris [4]. Although the location and timing of WD varies slightly according to the organism and type of injury, the general process is rapid and is conserved across vertebrates [4, 5]. Importantly, these debris will prevent new axonal growth if not properly cleared [6].

1.3 Extrinsic barriers to regeneration

The debris generated by WD secrete inhibitory proteins that produce sustained inhibition of regeneration [7, 8]. These proteins, generally produced from the breakdown of myelin, include: NogoA, myelin-associated glycoprotein, and others [9-11]. Although inhibitory proteins are present in both the central and peripheral nervous systems, the PNS is able to clear the debris [12]. In the PNS, macrophages and other phagocytic cells gather to clear the myelin sheath and other debris resulting from degeneration [13]. This occurs rapidly in the PNS. In mice, the initial clearance phase in the PNS takes around 72 hours and is complete in 1-2 weeks [14]. Conversely, this process is very slow in the CNS and it can take years to fully clear the debris [3, 14]. Further, the CNS forms a glial scar made up of reactive astrocytes, cytoskeletal elements, and other debris. Although helpful for stabilization of the CNS after injury, this scar presents a physical barrier across which regenerating axons cannot grow [15, 16].

Slow axon clearance is one of the main extrinsic limitations of the CNS. The sustained presence of regeneration inhibitors is prohibitive for regeneration. In the newt, which exhibits robust axonal regeneration, even in the CNS, the phagocytic-immune response to CNS injury is as rapid as the mammalian response to PNS injury [17]. This rapid immune response clears the way for regeneration of the injured CNS axons. This point is further illustrated by transplantation experiments. First, when PNS neurons are exposed to the CNS environment, reactive oligodendrocytes, the myelinating cells of the CNS, induce rapid, sustained loss of

neurite outgrowth potential [18]. Schwann cell transplants, the myelinating cell of the PNS, are sufficient to significantly increase axonal regeneration of CNS neurons [19-21]. Further, Schwann cell grafts can remyelinate axons, restoring conductive communication in the CNS [22].

These experiments, taken together, suggest that the external environment is an essential part of the regenerative mechanism of the PNS. However, transplantation experiments have shown that most CNS neurons are unable to regenerate, even in the permissive context of the PNS. Those that do, are unable to reach the full functional recovery seen in the PNS [20, 21, 23]. Clearly, intrinsic factors are also an important component of regeneration.

1.4 Intrinsic programs of regeneration

Although there is diversity in response to injury amongst neurons, PNS and CNS neurons generally respond very differently to injury. First, in the neuronal cell body of both systems, injury triggers swelling, displacement of the nucleus, localization of the Nissl substance, and loss of synaptic function. Regeneration-competent PNS neurons become hypertrophic and upregulate overall metabolism, including protein translation, while regeneration-noncompetent CNS neurons either display no obvious physiological reaction, or decrease in volume and reduce dendritic number [24-26]. In the PNS, injury signals a change in intracellular ion concentrations and propagates a retrograde calcium wave from the point of injury to the cell body [27]. This signal, which propagates at 1mm/minute in rodents, is

responsible for the upregulation of protein translation and the reorganization of the cytoskeleton, as discussed above. In addition, the calcium wave signals formation of a growth cone-like structure, a component initially seen during development and which is essential to axon extension [28-30]. This structure forms within 24 hours and regrowth begins soon after [31, 32]. In contrast, the injured ends of many CNS axons retract and form a dystrophic bulb that is prohibitive for regeneration, even in the face of a regeneration-permissive environment [32, 33].

1.5 Regeneration associated genes

Essential to the success of the peripheral response is the activation of a genetic pro-regenerative program, known to involve *de novo* transcription of genes silenced in the basal state [34]. Genes that are transcribed in this manner, essential for PNS regeneration, are commonly known as RAGs (regeneration associated genes). The first genes identified from this group, the GAP family (including GAP-43), was found to have little expression in the injured CNS but robust upregulation in the PNS following injury, and to be essential to regeneration [35]. To date, the list of annotated, experimentally confirmed RAGs has grown to over 300 [36]. Each gene added to the list generally follows the same framework as described above and, in addition, may also induce CNS regeneration through overexpression of the RAG (for examples, see: [37-39]). Many RAGs are transcription factors and therefore orchestrate a larger genetic transcription response [38]. For this reason, work in the field has focused on closely approximating the complete transcription program elicited in the PNS [36]. For

example, knockout (KO) of KLF4, a transcription factor with numerous targets, was found to increase regeneration in the optic nerve [40]. Generally, however, any genetic manipulation has focused on the modification of only a handful of genes [41-43].

Together, these studies make it clear that regeneration in the peripheral nervous system requires a concerted, global, and sustained change that regulates activities as diverse as microtubule reorganization and *de novo* gene transcription. This suggests two things: first, that the peripheral nervous system might be a good starting place for unraveling the problem of regeneration in all neuronal systems; and second, that any significant change must originate with global regulatory mechanisms.

CHAPTER 2 - Epigenetic regulation of regeneration

2.1 Introduction

The epigenome is a dynamic system. Epigenetic molecular changes, which can be heritable, regulate transcription without altering the genetic code itself [44]. Generally, these changes are divided into two categories: DNA methylation and histone modifications. In addition to other regulatory proteins, such as the SWI/SNF remodeling complex, these mechanisms regulate gene transcription.

2.2 Chromatin and histone modifications

DNA is organized in a hierarchical manner, packaged to be read and interpreted appropriately for the cell's needs. During normal cellular activity, the 2nm DNA helix is wrapped around nucleosomes to form the 10nm 'beads-on-a-string' structure. The DNA is organized for active use or inactive storage with additional proteins, such as the linker H1 protein [45]. Nucleosomes are made up of an octet of histones, two copies each of H2A, H2B, H3, and H4. Each of these histones has an N and C-terminal tail whose amino acid residues, such as arginine and lysine, can be modified to alter the chromatin structure, and thus the level of transcription [46].

These modifications can either condense DNA into transcriptionally inaccessible heterochromatin or transcriptionally active euchromatin. The cell interprets the pattern of histone modifications and makes appropriate changes. This histone modification pattern, called 'the histone code', is complex and still not well

understood [47]. However, in general, histone methylation silences transcription while histone acetylation produces active transcription [48].

2.3 DNA methylation

Like histones, the DNA itself can also be modified to alter transcription [49]. A methyl group can be added to cytosine, generally in, but not exclusively limited to, CpG sites [50, 51]. This covalent modification of the 5-carbon position of cytosine produces 5-methylcytosine (5mC). Methylated cytosine presents a physical impediment to the binding of the transcription machinery and interacts in a cooperative manner with histone modifications to coordinate transcriptional changes [52].

2.4 Modifications are dynamic and fundamental

The epigenetic machinery is made up of ‘writers’, which apply the modifications, ‘readers’, which interpret the modifications and direct the cell accordingly, and ‘erasers’, which remove existing modifications. Histone modifications are added by a family of histone acetyltransferases (HATs), histone methyltransferases (HMTs), and others according to the modification being added. These modifications can be removed through a related family of proteins such as histone deacetylases (HDACs) and histone demethylases (HDMs), respectively [53]. Readers, an equally diverse family of proteins, have modification binding domains which can bind directly to and recruit other components, such as the polycomb repressive complex and Trithorax active complex, to produce the required regulatory effect

[54, 55]. DNA methylation is added by DNA methyltransferases (DNMT) and removed by Ten-eleven translocation (TET) enzymes [56, 57]. The family of DNA methylation readers is diverse, but all contain a methyl-binding domain [58].

During development, DNA is selectively and progressively silenced as the cell moves along its differentiation path [59]. This tightly controls transcription to a situation-appropriate level. This type of epigenetic activity is generally considered to be stagnant, changing in only very limited cases, particularly in regards to post-mitotic cells [60]. However, the moment-to-moment needs of a cell change drastically, and the dynamic nature of the epigenome is equipped to handle these changes in transcriptional demand. DNA methylation was originally hypothesized to regulate gene expression as early as the 1970s, but was thought to be removed passively, through cell division. However, it was recently discovered that methylation can be selectively targeted and removed through iterative oxidation followed by base excision repair [57, 61, 62]. Similarly, histone modifications can be removed quickly and efficiently [63]. The dynamic nature of the epigenome is an important component of cellular plasticity and is essential for responding to environmental changes, such as injury.

2.5 Neuroepigenetics

The regulation of large transcriptional programs is essential for the normal function of many systems (for example see: [64]). The tight regulation of the epigenome is particularly relevant for neurons, post-mitotic cells which must respond delicately

to insult [65]. Unsurprisingly, there is a significant epigenetic contribution to the neural transcriptome landscape [66]. Developing neurons have a significantly different transcriptional load than mature neurons. 5-hydroxymethylcytosine (5hmC), an oxidative product of 5mC, tends to increase as development progresses and decrease during dedifferentiation [67, 68]. As the cell develops, transcriptional programs associated with growth and differentiation are silenced and, in the CNS, intrinsic growth capacity declines [60, 69, 70]. This tight regulation is essential to proper growth and development. For example, a mutation in any of the three DNMTs is incompatible with life [71, 72]. Scenarios in which the mutation only occurs in a neuronal system still have profound consequences on proper neural development [73]. In mature neurons, transcription is also regulated by epigenetics. For example: growth arrest and DNA-damage-inducible protein 45β (GADD45β) promotes adult hippocampal neurogenesis [74]. Changes in the epigenome are essential to neural plasticity, such as in learning and memory formation or in acute activation of neural pathways [75, 76].

2.6 Histone acetylation and regeneration

Several recent studies reveal the specific role of histone modifications in regeneration. First, overexpression of the acetyltransferase p300 increases CNS regeneration [77]. This connects the high demand of newly synthesized RNAs with the role of histone acetylation in the activation of gene transcription [34, 48]. Next, nuclear export of HDAC5 (a histone deacetylase) is essential for the accumulation of acetylation in the PNS after injury. If HDAC5 is modified and prevented from

exiting the nucleus, regeneration cannot proceed [78]. Further, histone H4 is hypoacetlylated in the CNS. Pharmaceutical-facilitated acetylation accumulation also increases regeneration in the CNS [79]. These studies highlight the role of activating histone marks in regeneration. However, histone modifications are only one component of the epigenetic machinery. Modification of DNA demethylation also allows the upregulation of genes through the removal of repressive methylation [57, 80].

PNS regeneration requires complete transcriptional reprogramming to meet the demands of the injured neuron. The epigenome, as a dynamic, crucial regulatory system is equipped to meet these needs. In this study, we investigate the role of DNA methylation in mediation of the pro-regenerative state of PNS injury response.

CHAPTER 3 - RESULTS

3.1 Dorsal Root Ganglion

The peripheral nervous system demonstrates robust, sustained regeneration after injury. Therefore, we chose to use this system to investigate the role of DNA methylation in injury response. The dorsal root ganglion (DRG) is a well-established model of PNS injury [34]. The DRG is a bundle of sensory neuronal nuclei that lies just off of the spinal cord. DRG neurons are pseudo-bipolar. They possess two axonal branches, one, which projects distally, reaching the far extremities to provide sensory feedback, and one, which projects proximally, reaching into the spinal cord. The sciatic nerve, which projects from the L4/L5 vertebrae in mice, is composed of both motor neurons, whose cell bodies lie inside the spinal cord, and sensory neurons from the DRG [81] (Figure 3.1). The sciatic nerve is relatively superficial and can be exposed and injured with only minor invasion [82]. In this study, we performed a sciatic nerve lesion (SNL) injury via crush (Figure 3.2). Molecular analysis was completed in the DRG, and assessment of regeneration was completed in the sciatic nerve.

3.2. Demethylation following injury

First, we first determined whether DNA methylation was involved in injury response. We performed SNL surgery on wild type (WT) mice, removed the DRG at one day post-SNL (SNL D1), and extracted RNA from the whole DRG. In each mouse, we performed SNL on one side, and kept the contralateral side naive as an internal control. We used qPCR to screen for known demethylation mediators:

Tet1-3, Apobec1-3, Gadd45a, Gadd45b, Gadd45g, and Tdg [83, 84]. Gadd45a, Gadd45g, and Tet3 were upregulated following injury (Figure 3.3). Gadd45a has previously been shown to regulate DNA demethylation, and can be induced by neural activity [74]. The observed upregulation of Gadd45a is consistent with previously published data [85].

3.3 Tet3 upregulation

The Tet family of enzymes consists of 3 members: Tet1, Tet2, and Tet3. Each of which can iteratively oxidize 5mC to return it to its unmodified cytosine state (Figure 3.4) [84]. Interestingly, Tet3, but not Tet1 or Tet2, is active in the DRG (Figure 3.3). This is true at both basal conditions and following injury, despite robust expression of all three Tets in the hippocampus (Figure 3.5). Tet3 is induced by SNL D1, reaches peak expression level at SNL D3, and has returned to basal levels by SNL D14 (Figure 3.6). We further investigated Tet3 expression using *in situ* analysis of DRG cross-sections to identify which cell type accounts for the observed transcriptional upregulation in the whole DRG. For this experiment, we used a transgenic reporter mouse line that expresses GCaMP3 from the endogenous Pirt locus. This line labels over 95% of neurons in the adult DRG [86]. Tet3 is neuron specific and its upregulation occurs at both the transcript and protein level (Figure 3.7, 3.8)

3.4 Retrograde signaling

It has been established that the injured axon signals the soma to activate a regenerative program via calcium retrograde signaling [87]. For this reason, we thought it likely that calcium signaling was involved in Tet3 upregulation. To test this, we measured Tet3 levels after treatment with a calcium chelator and a CaMKII inhibitor, BAPTA-AM and KN93, respectively. Both inhibitors blocked the upregulation of Tet3 in the DRG while KN92, an inactive analog, did not (Figure 3.9). This is consistent with previously published data on histone modifications and regeneration [78].

3.5 Tet3 KD blocks demethylation

The demethylation of 5mC is one of the main roles of enzymes in the Tet family (Figure 3.4). Therefore, we asked whether the upregulation of Tet led to an increase in 5hmC, an oxidative derivative of 5mC (Figure 3.4). 5hmC increases in Pirt-GCaMP3^{+} DRG neurons at SNL D1 (Figure 3.10). Further, the time course of 5hmC corresponds to the time course of Tet3; 5hmC levels are higher at SNL D1, peak at SNL D3, and return to normal by SNL D14 (Figure 3.11). This suggests that Tet3 is involved in the global demethylation of 5mC observed following injury.

To determine whether the time course association of 5hmC and Tet3 is correlative or causative, we designed an adeno-associated virus (AAV) to target and knockdown (KD) expression of Tet. The virus contained both a previously characterized small hairpin RNA (shRNA), as well as a GFP reporter [88]. We

delivered the virus via intrathecal injection to WT mice (Figure 3.12). By injecting between the 4th and 5th lumbar vertebra, the virus can disseminate into the corresponding DRG. Both the Tet3 KD (Tet3-shRNA) and control (ctrl-shRNA), containing a scrambled shRNA, effectively labeled over 70% of L4/L5 DRG neurons (Figure 3.13). Tet3 KD eliminated the SNL-mediated increase in 5hmC, suggesting that Tet3 is directly involved in injury-related global demethylation (Figure 3.14, 3.15, 3.16).

3.6 RAG expression

As described above, RAGs are essential for regeneration in the PNS, and, therefore any comprehensive pro-regenerative program will likely regulate RAGs [34]. We next investigated whether Tet3 upregulation was associated with RAG expression in vivo. For this, we compared RAG levels in Tet3-shRNA treated animals to RAG levels in ctrl-shRNA treated animals. In the ctrl-shRNA, RAGs had low basal expression and upregulation following injury. However, Tet3 KD blocked the expression of several RAGs including: ATF3, Smad1, STAT3, and c-Myc [89, 90](Figure 3.17). Additionally, Tet3 altered the basal expression of some RAGs (Figure 3.15). Together, this data presents a model wherein Tet3 regulates expression of RAGs both under naive conditions as well as in response to injury.

3.7 ATF3 expression

In order to interrogate the effect of Tet3 on RAG expression more fully, we chose one gene, ATF3, to explore further. ATF3 is one of the most robustly upregulated

genes following SNL and has the capacity to increase CNS regeneration [38, 91]. Immunohistochemical (IHC) staining of ATF3 in the DRG was consistent with previous publications. Importantly however, Tet3 KD attenuated the normal upregulation of ATF3 (Figure 3.18). There is little to no ATF3 expression through SNL D7, suggesting that Tet3 blocks expression of RAGs rather than delaying their expression (Figure 3.18). Finally, retrograde signaling, as assessed though quantitative IHC staining of c-jun, is intact (Figure 3.19) [87]. This suggests that Tet3 does not block all injury-induced signaling, instead acting in a more precise manner.

3.8 RAG demethylation

Next, we next wanted to determine whether the Tet3-mediated upregulation of RAGs occurred via demethylation. Because the DRG is 90% non-neuronal cells, we enriched for neurons using a sucrose cushion [92, 93]. First we first screened ATF3 for methylated sites using methylation sensitive restriction enzymes (MSRE) which can identify 5mC and 5hmC sites within the sequence CCGG [94]. We determined that, although the promoter was relatively free of methylation, distal enhancer regions were hypermethylated (Figure 3.20). Enhancer regions modulate transcription through the binding of various proteins, and are particularly important centers for methylation [95]. At SNL D1, several sites, including distal enhancer regions, exhibited a decrease in methylation (Figure 3.20). We also screened c-Myc, a gene recently shown to be an important RAG whose overexpression can lead to gains in CNS regeneration [96]. Similar to ATF3, c-Myc

had a hypomethylated promoter, and hypermethylated enhancer regions that were demethylated following injury (Figure 3.21). We confirmed the MSRE results with bisulfite sequencing [97]. First, we used FACS (fluorescence-activated cell sorting) to sort neuronal nuclei using fluorescence-conjugated NeuN. Distal enhancers of ATF3 exhibited demthylation following injury, while GAP43 remained methylated (Figure 3.22, 3.23). Therefore, demethylation is a tightly regulated, region specific process.

Although the data above make it clear that Tet3 is important for the upregulation of RAGs, which occurs concomitant with demethylation, further testing was necessary to directly connect Tet3 regulation with the demethylation event. Therefore, we performed bisulfite sequencing on Tet3 KD samples. We altered our Tet3 AAV to express a variant GFP, H2B-GFP, which is detectable while sorting nuclei with FACS. We FACS-purified eight groups of $NeuN^+$ nuclei: GFP^- uninfected neurons or GFP^+ neurons expressing either ctrl-shRNA or Tet3-shRNA, under either the naive condition or at SNL D1 (Figure 3.24, 3.25). GFP^- cells act as a natural internal control. In the distal enhancer 1 (DE1) region, a demethylation event occurred at SNL D1 in ctrl-shRNA condition, whether GFP^+ or GFP^-, as well as in the Tet3 uninfected GFP^- condition. However, Tet3-shRNA GFP^+ neurons are not demethylated following injury (Figure 3.24, 3.25). Thus, Tet3 is essential for the demethylation event observed in certain RAGs following injury.

3.9 Tet3 recruitment

ChIP-qPCR (chromatin immunoprecipitation-qPCR) using an antibody against Tet3 [98] reveals that there is increased Tet3 binding to the ATF3 DE1 locus, a region which exhibited a significant demethylation event, but not to GAP43 loci, which remained methylated after injury (Figure 3.26). This indicates that PNS injury recruits Tet3 to certain methylated regions of RAGs, leading to the demethylation and subsequent upregulation of those RAGs.

3.10 Axon regeneration

Our data suggest a model wherein Tet3 is recruited via retrograde signaling to hypermethylated regions of RAGs. This Tet3 recruitment allows for the demethylation and, therefore, upregulation of those RAGs. Given the essential role of RAG expression in regeneration, we hypothesized that Tet3 KD was likely to have profound consequences for functional regeneration. To test this, we competed a functional assessment of the effects of the Tet-shRNA.

First, we used an *in vitro* neurite outgrowth assay to measure changes in neuron growth following Tet3 KD. Purified, primary neurons from adult mouse DRGs were disassociated and plated. These cultures were infected with AAV2/9 which co-expresses GFP and an shRNA against Tet1, Tet2, or Tet3, followed by re-plating, which mimics axotomy (Figure 3.27). We found that Tet3 KD reduced both the number and the total neurite length of neurite-bearing neurons, while Tet 1 and Tet

2 KD were indistinguishable from the control (Figure 3.28, 3.29). *In vitro*, Tet3 prevents extension of DRG neuron axons.

Next, we used the AAV Tet3 KD *in vivo*. We delivered the virus via intrathecal injection, as described above. SNL surgery was performed, and whole sciatic nerves were removed at SNL D3 and SNL D7. We assessed the extent of regeneration using SCG10, which stains regenerating axons [99]. We quantified axons in two ways. First, we took longitudinal sections and assessed regeneration by fluorescent intensity (Figure 3.30). At SNL D3, sciatic nerves from ctrl-shRNA treated animals had extended significantly further than those from Tet3-shRNA treated animals (Figure 3.30, 3.31). Because degeneration is still occurring at SNL D3, we also removed sciatic nerves at SNL D7, when degeneration is complete and all debris has been removed [100]. We cross-sectioned the sciatic nerves at 1mm intervals (1mm-6mm) along the sciatic nerve, using -1mm to normalize, and quantified the number of regenerating GFP^+ axons in the coronal sections (Figure 3.32, 3.33). Tet3-shRNA treated animals exhibited a significant regeneration deficit as compared to ctrl-shRNA treated animals (Figure 3.33, 3.34, 3.35). Almost half (43%) of Tet3 KD neurons were unable to extend their axons past 1mm, while only 17% of ctrl-shRNA neurons did not extend past 1mm. Conversely, over 62% of ctrl neurons extended axons over 6 mm from the lesion site but only 33% of Tet3 KD neurons were able to reach this distance (Figure 3.34, 3.35). We observed no other phenotypic differences between the Tet3 and ctrl-shRNA samples, including both

morphology and neuronal death rate, ruling out the possibility that regeneration differences were due to cellular instability or loss (Figure 3.36, 3.37).

3.11 Sensory recovery

The fundamental measure of regeneration in the DRG is recovery of sensory input and processing. In mice, sensory recovery occurs at 2-3 weeks post-SNL, as the sensory neurons begin to re-innervate the skin [101]. To measure the extent of re-innervation, we took skin biopsies from the mouse hindpaw following SNL, and stained for axons using PGP9.5 (Figure 3.38, 3.39). Under naive condition, axons of both the Tet3 and ctrl-shRNA neurons fully extend into the epidermis (Figure 3.40). At SNL D7, all mature, preexisting axons from both the Tet3 and the ctrl-shRNA neurons had degenerated (Figure 3.39). By SNL D21, the ctrl-shRNA neurons had begun re-innervating the epidermis, while Tet3-shRNA neurons were mostly non-existent in the skin samples and unable to pass into the dermis (Figure 3.40, 3.42). We assessed the extent of re-innervation by dividing the dermis and epidermis into three layers and quantifying the number of nerve fibers in each layer (Figure 3.41). In both the ctrl and Tet3-shRNA groups, naive axons were morphologically similar (Figure 3.40). We did not detect a difference in the innervation of preexisting axons in the naive samples (Figure 3.42). However, in every zone, the Tet3-shRNA SNL group had significantly fewer axons (Figure 3.42). Thus, Tet3 is required for both regeneration as well as re-innervation into the distal target areas.

Given that Tet3-shRNA is required for re-innervation of the epidermis, we expected that Tet3-shRNA mice would exhibit drastic deficits in sensory recovery. To evaluate this, we employed a behavioral test which quantifies the latency of hindpaw withdrawal [102]. At intervals between SNL D7 and SNL D21, we measured the time for hindpaw withdrawal from exposure to a radiant heat source. We first tested the mice before injury to get a baseline reading for the naive withdrawal time, and normalized each mouse to their own baseline time. Naive mice from both treatment conditions responded similarly, removing the paw quickly (Figure 3.43). At SNL D7, latency times were also equivalent. Both groups took considerably longer to respond to the stimulus than prior to injury (Figure 3.43). By SNL D21, the ctrl-shRNA group had begun to recover, but the latency deficit of the Tet-shRNA treatment mice persisted throughout the time course (Figure 3.43). Together, these data reveal that Tet3 is an essential component of functional recovery in the PNS exhibits.

3.12 TDG

Although demethylation is one of the Tet proteins' major roles, it also has many noncanonical activities [103-105]. In addition, 5hmC can independently be used as a signaling molecule independently [49, 106, 107]. However, our data suggest that the primary role of Tet3 in regeneration is that of demethylation, with 5hmC as an intermediate of the active demethylation process (Figure 3.4). In order to clarify this role, we also examined the influence of thymine DNA glycosylase (TDG) in regeneration. TDG functions together with the base excision repair machinery to

restore the oxidative products of demethylation, 5caC (5-carboxylcytosine) and 5fC (5-formylcytosine), to unmodified cytosine [62, 108].

We hypothesized that, while Tet3 KD led to a decrease in 5hmC, TDG would lead to an increase in 5hmC, as the cell is unable to fully demethylate oxidative intermediates (Figure 3.4). We engineered a TDG KD AAV, with the same backbone and GFP expression of the Tet3 KD virus and delivered it via intrathecal injection for *in vivo* analyses (Figure 3.12). Consistent with previous data, TDG KD increased the level of 5hmC in the DRG (Figure 3.44, 3.45) [62, 109]. Similar to the Tet3 KD, TDG KD attenuated expression of ATF3, both at D1 and D7 post SNL (Figure 3.46, 3.47). ATF3 still retained some expression in the DRG following TDG KD, in contrast to the fully-attenuated levels of ATF3 in the Tet3 KD (Figure 3.47). This is likely because 5caC and 5fC do not block transcription as 5mC and 5hmC do, but rather slow and reduce transcription [110]. qPCR analysis revealed that the effect of TDG KD on RAG expression is analogous to that of Tet3. Just as in the Tet3 KD animals, SNL-induced transcription is blocked for many RAGs following TDG KD, but the expression of some, such as GAP43, do not appear to be under the control of the demethylation pathway (Figure 3.48). TDG KD also blocks sciatic nerve regeneration, as assessed by coronal sectioning of the sciatic nerve (Figure 3.32, 3.49, 3.50). We verified this result using $TDG^{f/f}$ KO mice (Figure 3.51, 3.52). These data corroborate the model, in which demethylation is the primary role of Tet3-mediated RAG expression.

3.13 Application to the CNS

The PNS is an ideal system to identify regeneration factors. As such, we were interested in the role of DNA demethylation in the CNS. To investigate this, we used a recent model which increased CNS regeneration, PTEN KO, to observe the effect of Tet KD [111]. We used the same Tet1, Tet2, and Tet3 shRNAs as above, but modified them to target retinal ganglion cells. Tet3 is the only DNA demethylase expressed in the PNS, but Tet expression is tissue and context dependent (Figure 3.5). Tet1-shRNA treatment reduced the regeneration gain of PTEN KO mice (Figure 3.53, 3.54). This indicates that Tet1 is essential to the CNS regeneration program induced by PTEN KO. Further, only Tet1 mitigated regeneration in the CNS, this suggests that specific expression of the correct set of genes will be essential to reprogramming CNS neurons for regeneration.

Figure 3.1

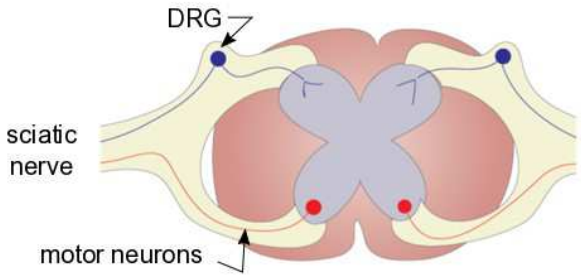

Figure 3.2

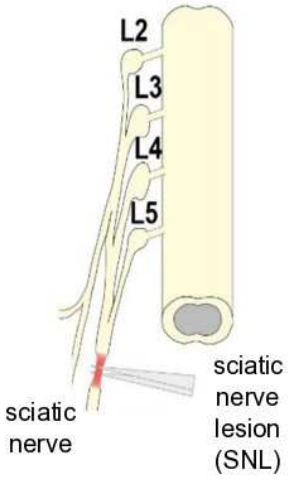

FIGURE 3.1: DRG schematic*: Schematic drawing of the DRG structure which lies just outside of the spinal cord but is protected by the vertebrae. Each vertebra protects its corresponding DRG. Sensory neuron cell bodies are housed in the DRG, while motor neuron cell bodies are housed within the spinal cord.*

FIGURE 3.2: SNL schematic: *The L4/L5 DRG, together with the motor neurons make up the sciatic nerve. SNL surgery is delivered at mid-thigh level.*

Figure 3.3

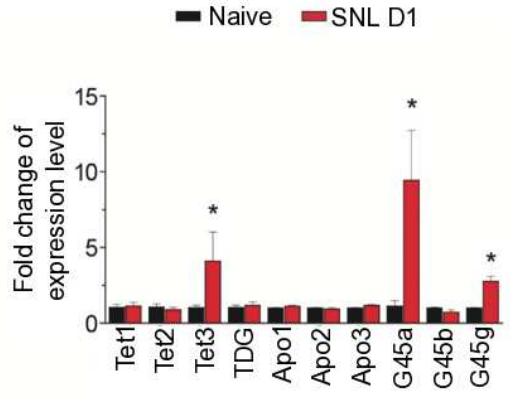

Figure 3.4

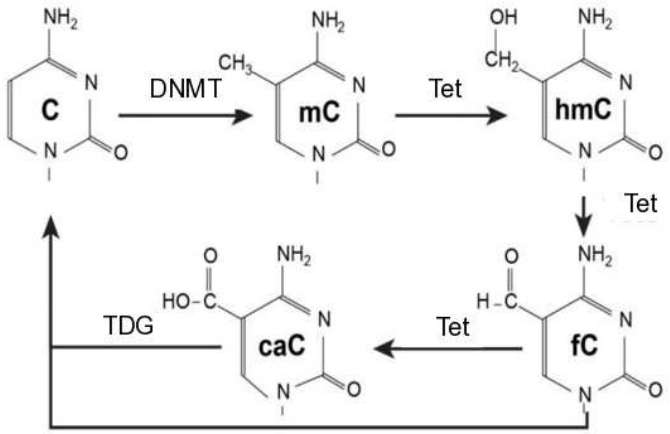

FIGURE 3.3. qPCR of epigenetic regulators in DRG: *Analysis of expression of some known RAGs. The mRNA expression was assessed by qPCR at SNL D1 and compared to the naive group. Values represent mean ± SEM (n = 3 for each group; ***p < 0.001; *p < 0.05; n.s. p > 0.1; two-way ANOVA).*

FIGURE 3.4. Methylation pathway: *A schematic diagram illustrating known molecular mediators of active DNA demethylation.*

Figure 3.5

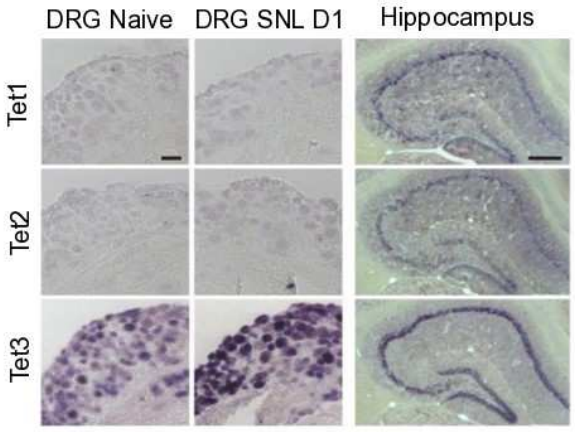

Figure 3.6

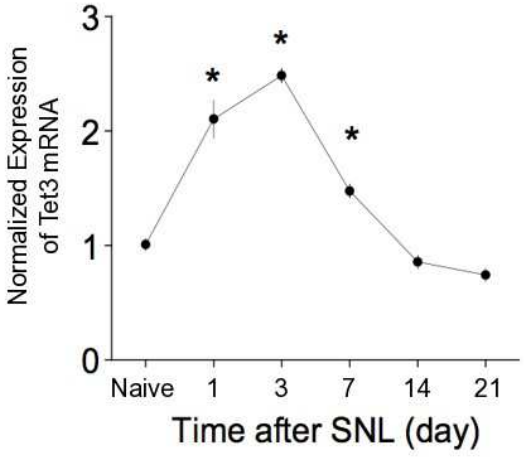

FIGURE 3.5. TET in situ: *In situ hybridization of Tet1, Tet2 and Tet3 in naïve and SNL D1 DRGs and in the adult mouse hippocampus (as a positive control). Scale bars: 50 µm*.

FIGURE 3.6. qPCR time course of TET3 expression: *Time course of Tet3 induction in after SNL in DRGs by qPCR analysis. Values represent mean ± SEM (n = 3 for each group; *p < 0.05; two-way ANOVA).*

Figure 3.7

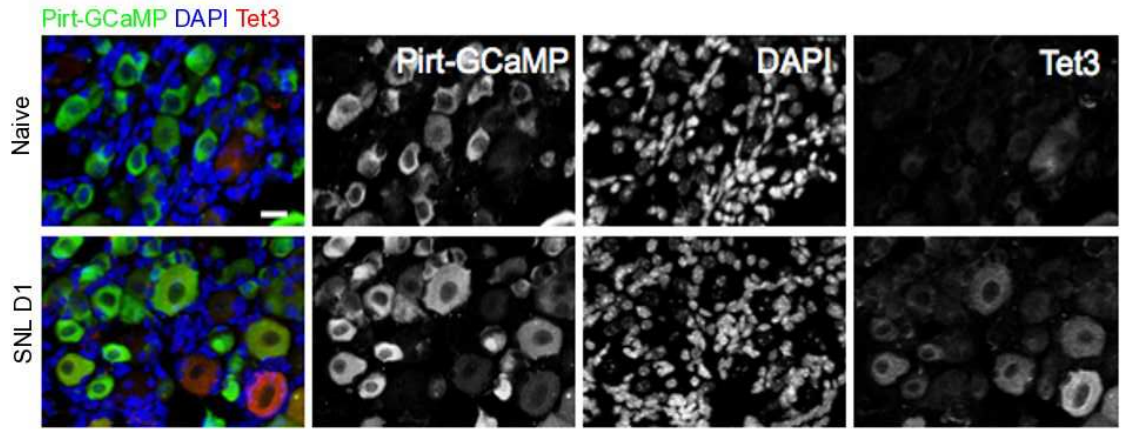

FIGURE 3.7. TET3 in situ, GFP IHC: *Sample confocal images of Tet3 in situ, GFP immunostaining, and DAPI of L4 DRGs in adult Pirt-GCaMP3 neuronal reporter mice under naive conditions and at SNL D1. Scale bar, 20 mm.*

Figure 3.8

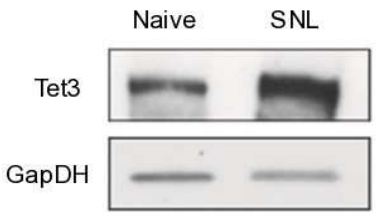

Figure 3.9

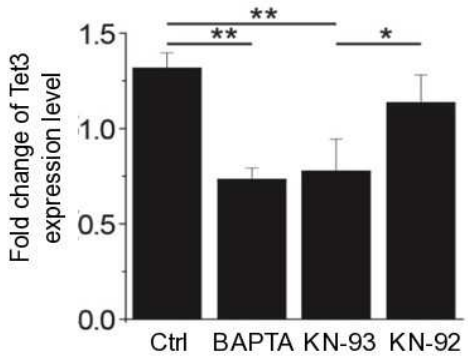

FIGURE 3.8. TET western blot: *Sample western blot image of Tet3 expression levels in DRGs under the naive condition and at SNL D1.*

FIGURE 3.9: Pharmacological study of retrograde signaling: *Signaling mechanism underlying injury-induced Tet3 induction. Adult DRGs were removed from the animals and treated with different pharmacological agents, BAPTA-AM (50 μM), KN92 or KN93 (10 μM) for 1 hr, followed by analysis of Tet3 expression by qPCR. Values represent mean + SEM (n = 4-6 each; ** P <0.01; *P < 0.05; ANOVA).*

Figure 3.10

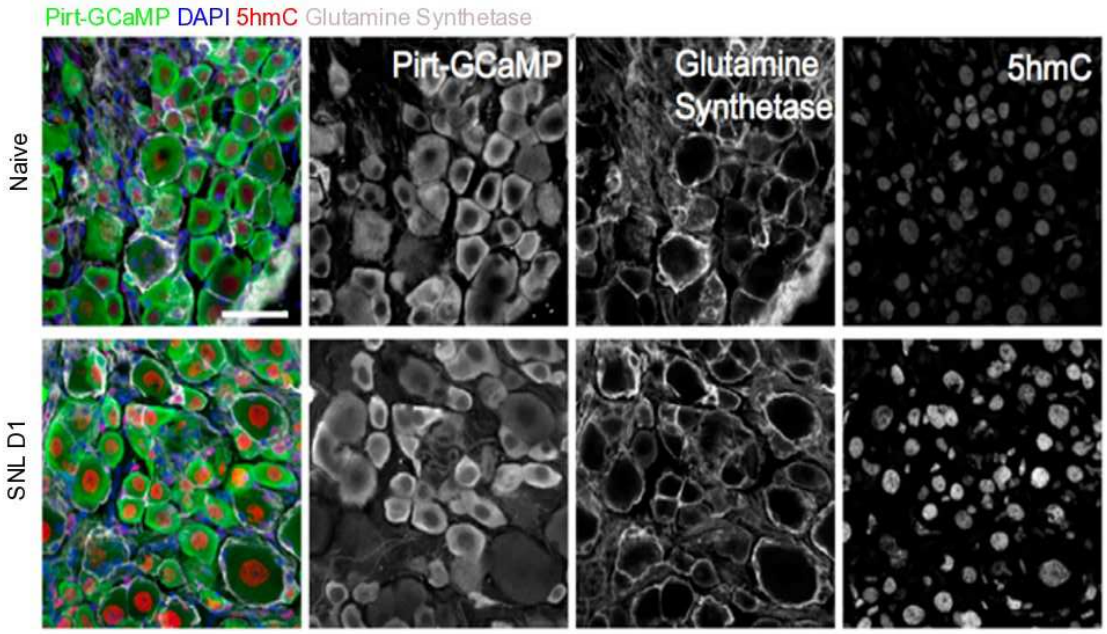

FIGURE 3.10. 5hmC IHC: *Sample confocal image of immunostaining for GFP, 5hmC, glutamine synthetase (GS), a marker for glia, and DAPI in DRGs of adult Pirt-GCaMP3 neuronal reporter mice under naive conditions and at SNL D1. Scale bar, 50 mm.*

Figure 3.11

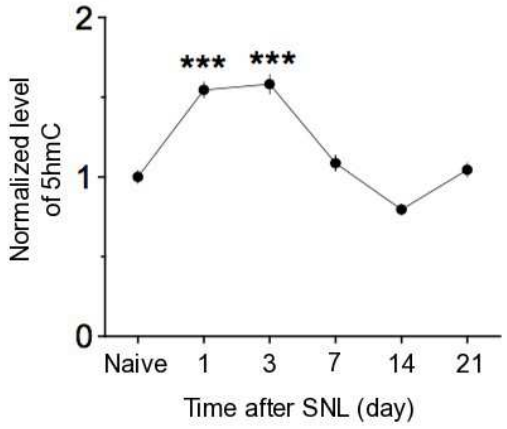

Figure 3.12

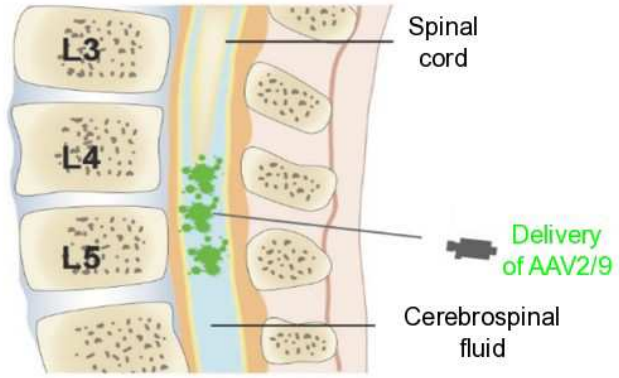

FIGURE 3.11. qPCR time course of 5hmC induction Quantification of 5hmC levels at different time points after SNL. The signal intensity in NeuN$^+$ neuronal nuclei of naive L4 DRGs was set as 1.0 and 100–180 neuronal nuclei from each condition in three independent experiments were quantified. Values represent mean ± SEM (n = 3 for each group; ***p < 0.001; two-way ANOVA).

FIGURE 3.12. Intrathecal injection schematic *A schematic diagram illustrating intrathecal injection of AAV to infect L4/5DRG neurons in adult mice in vivo.*

Figure 3.13

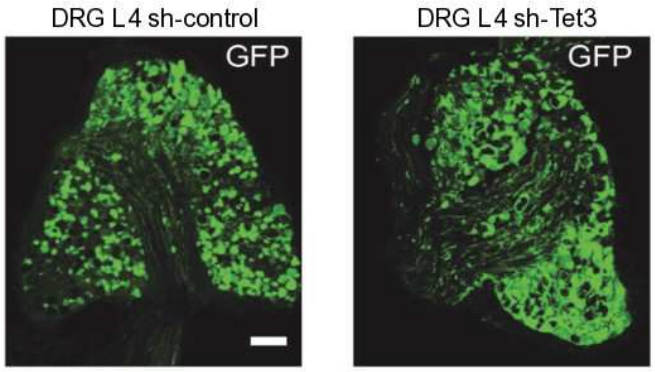

Figure 3.14

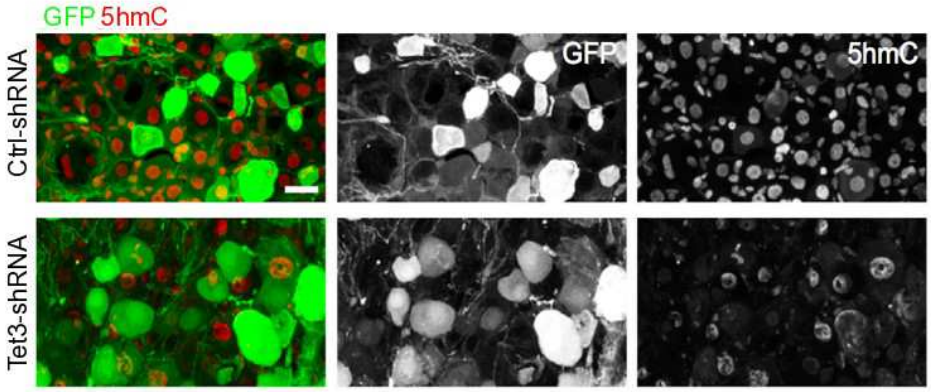

FIGURE 3.13. AAV efficacy: *Sample images of GFP-labeled neurons in DRGs at three weeks after AAV2/9 injection which expresses GFP together with either control shRNA or Tet3 shRNA. Scale bar: 50 μm.*

FIGURE 3.14. 5hmC IHC in Tet3 and ctrl-shRNA: *Sample images of immunohistochemical analysis of 5hmC levels in Ctrl and Tet3 KD DRG neurons under naive conditions and at SNL D1. Shown are sample images (scale bar, 20 mm)*

Figure 3.15

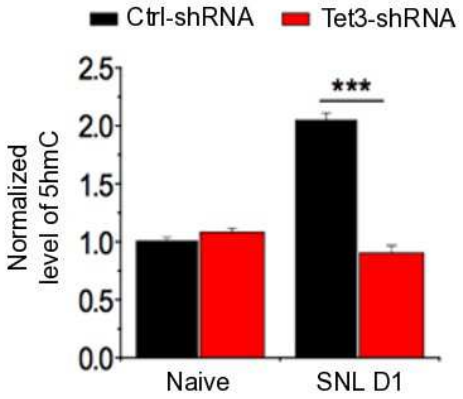

Figure 3.16

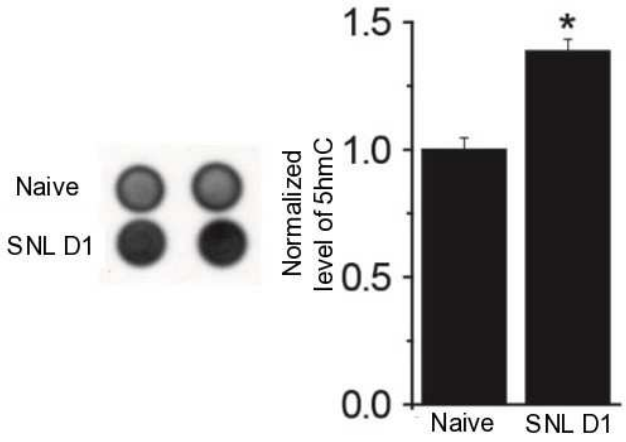

FIGURE 3.15. ***5hmC IHC in Tet3 and ctrl-shRNA quantification****: quantification. Values represent mean ± SEM (n = 3 for each group; ***p < 0.001; two-way ANOVA).*

FIGURE 3.16. Dot blot of global 5hmC levels: *Dot blot analysis of 5hmC levels in DRGs at SNL D1. Neuronal nuclei were enriched from naive and SNL injured DRGs via sucrose cushion followed by genomic DNA extraction. 100 ng DNA was spotted onto nitrocellulose membrane and 5hmC levels were detected with anti-5hmC antibody. Shown are sample images and quantification of the signal density. Values represent mean + SEM (n = 3; *P < 0.05; two-way ANOVA).*

Figure 3.17

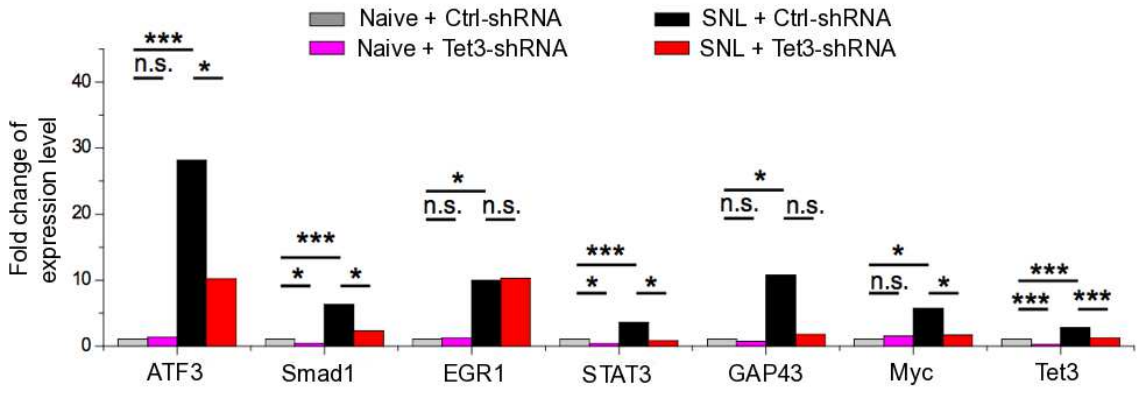

FIGURE 3.17. qPCR of RAG expression in Tet3 and ctrl-shRNA: *Analysis of expression of some known RAGs. The mRNA expression was assessed by qPCR at SNL D1 and compared to the Ctrl naive group. Values represent mean ± SEM (n = 3 for each group; ***p < 0.001; *p < 0.05; n.s. p > 0.1; two-way ANOVA).*

Figure 3.18

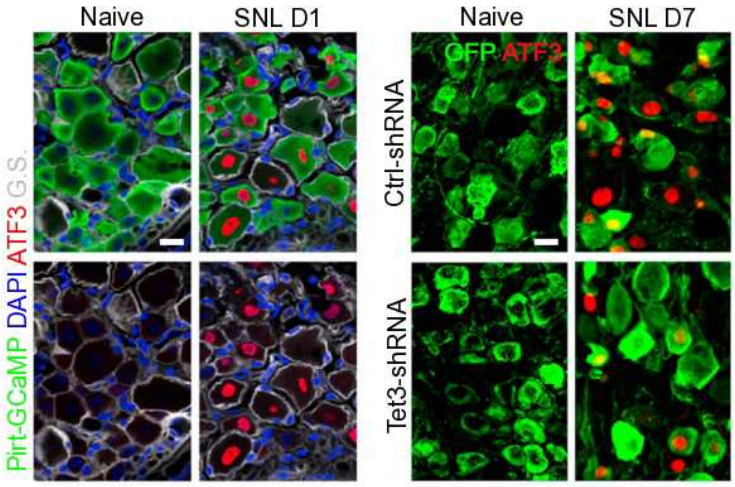

Figure 3.19

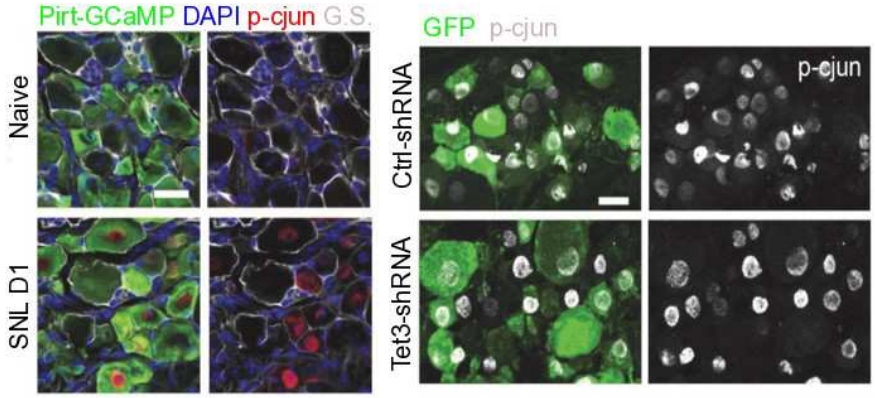

FIGURE 3.18. Tet3 IHC at SNL D1 and D7: *Assessment of ATF3 induction in Tet3 KD DRGs at SNL D1 and D7. Shown are sample images of immunostaining for GFP, ATF3, and Glutamine Synthetase (G.S.). in Pirt-GCAMP3 neuronal reporter mice and for ATF3 and GFP in normal mice*

FIGURE 3.19. p-c-jun IHC at SNL D1 in WT, Tet3 and ctrl-shRNA: *Sample images of immunostaining of phospho-c-Jun (p-cjun), GFP, Glutamine Synthetase (G.S.) in Pirt-GCaMP3 neuronal reporter mice, and GFP and p-jun in AAV-Ctrl and Tet3 shRNA treated DRGs*

Figure 3.20

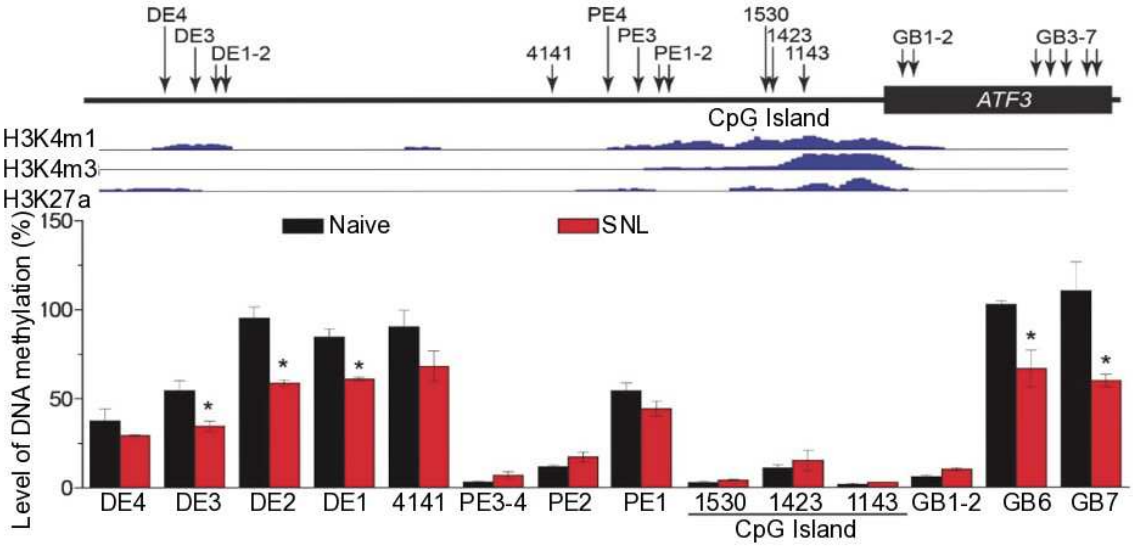

FIGURE 3.20. DNA methylation of ATF3: *DNA methylation analysis of the ATF3 genomic loci. Shown in the top panel is a schematic diagram illustrating the genomic region of ATF3 gene subjected to analysis. Shown in the middle panel is ChIP-seq data on three histone marks from ENCODE to identify genomic features of different genomic regions (DE: distal enhancer; PE: proximal enhancer; 4141: 4141 bp prior to ORF; GB: gene body; ENCODE-LICR-Histone Track, UCSC Genome Informatics). Shown in the bottom panel is a summary of DNA methylation levels at specific regions. Nuclei harvested from naive or SNL D1 DRGs were subjected to a sucrose cushion to partially enrich neuronal nuclei. Genomic DNA was then digested with either methylation-sensitive (HpaII) or insensitive enzymes (MspI). Primers spanning specific CCGG sites were used to amplify several putative regulatory regions of ATF3. Values represent mean ± SEM (n = 3; *P < 0.05; two-way ANOVA).*

Figure 3.21

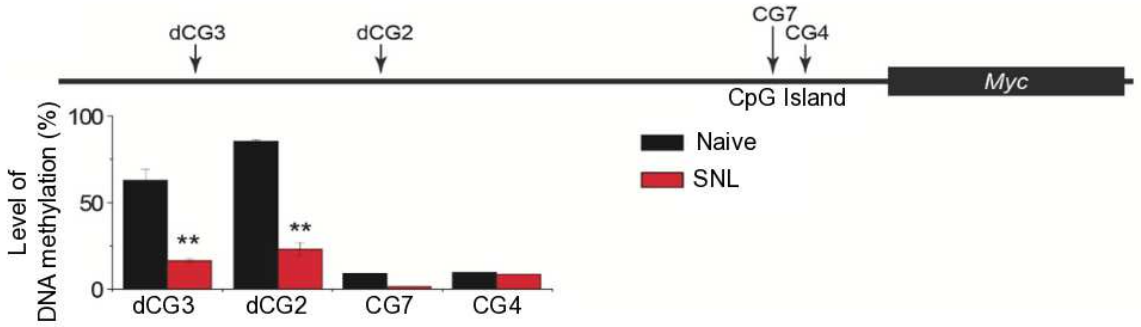

FIGURE 3.21. DNA methylation of c-Myc: *DNA methylation analysis of the c-Myc genomic loci, similar to Figure 3.20. Values represent mean ± SEM (n = 3; **P < 0.01; two-way ANOVA).*

Figure 3.22

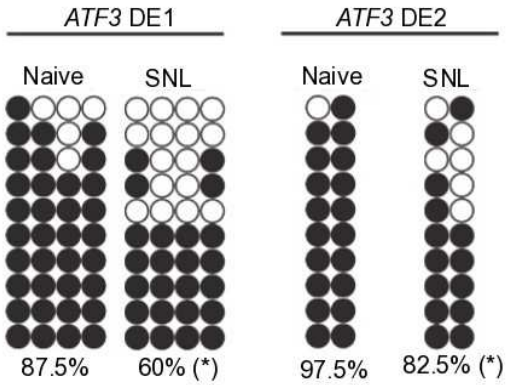

Figure 3.23

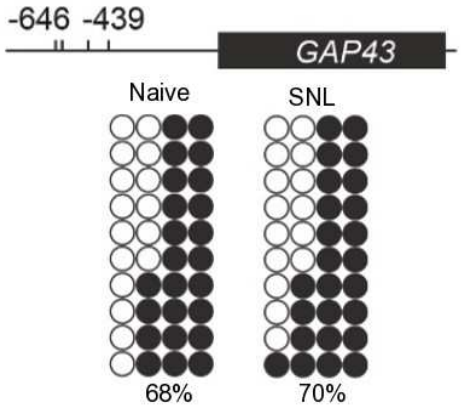

FIGURE 3.22. Bisulfite sequencing of ATF3: *Bisulfite sequencing analysis of ATF3 loci in naive DRG neurons and at SNL D1. NeuN$^+$ neuronal nuclei from L4 and L5 DRGs were purified by FACS. Each row represents one sequence read and each column represents an individual CpG site within the analyzed region. Dots represent methylated or unmethylated CpG sites. Numbers indicate the mean frequency of methylation at all CpG sites examined (*P < 0.05; Fisher's exact test).*

FIGURE 3.23. Bisulfite sequencing of GAP43: C-*myc methylation, similar to Figure 3.22*

Figure 3.24

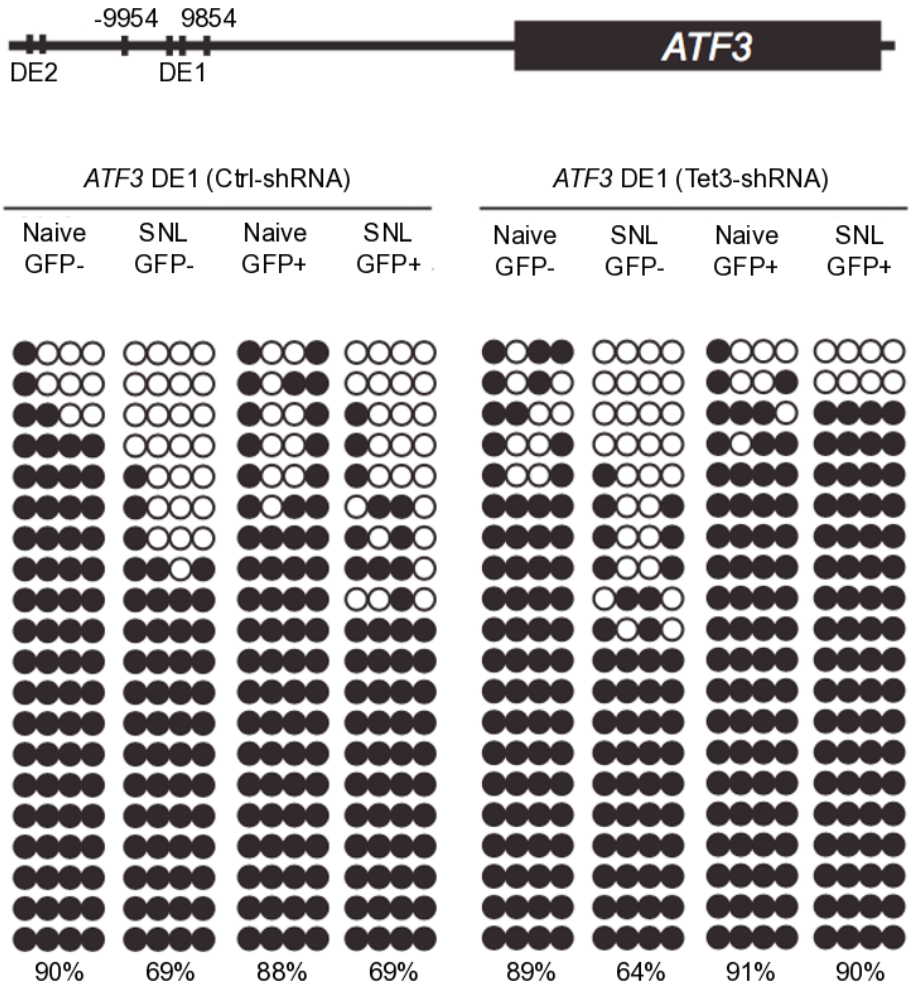

FIGURE 3.24. Bisulfite sequencing of ATF3 in Tet3 and Ctrl-shRNA: *Sample reads of individual alleles. Open circles indicate unmethylated cytosines and closed circles indicate methylated cytosines.*

Figure 3.25

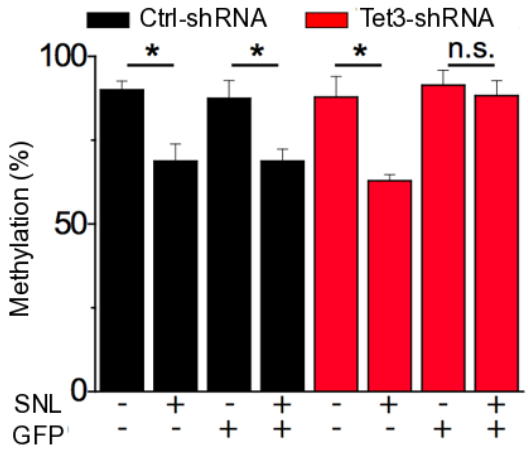

Figure 3.26

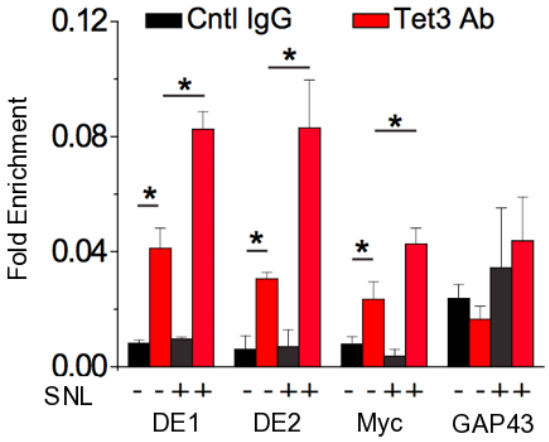

FIGURE 3.25. ATF3 bisulfite sequencing quantification: *Summary from three independent biological replicates with at least 20 alleles each. Values represent mean ± SEM (n = 3 for each group; *p < 0.05; two-way ANOVA).*

FIGURE 3.26. ChIP of Tet3 binding: *ChIP-qPCR analysis of Tet3 binding to different genomic regions that were also examined for DNA methylation levels.. Values represent mean ± SEM (n = 3 for each group; *p < 0.05; two-way ANOVA).*

Figure 3.27

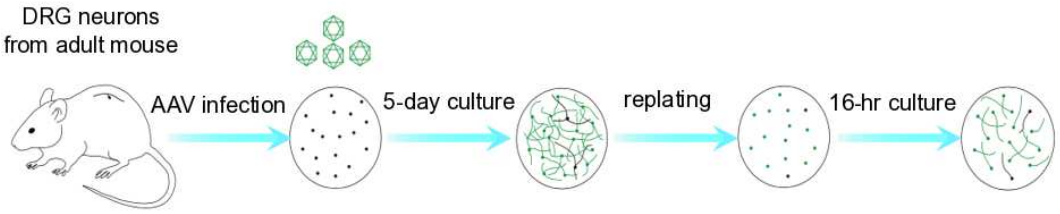

FIGURE 3.27. in vitro culture schematic: *Schematic diagram illustrating the DRG neuron replating assay for neurite outgrowth.*

Figure 3.28

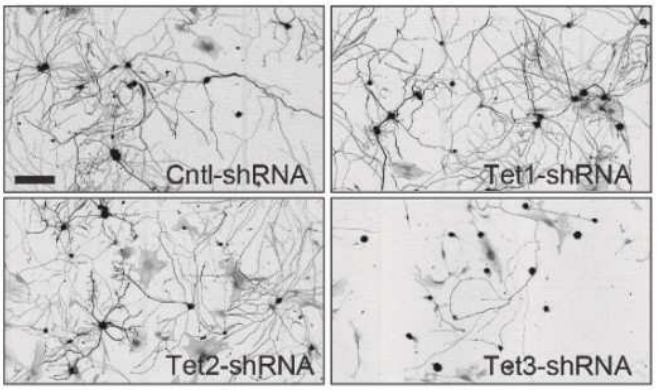

Figure 3.29

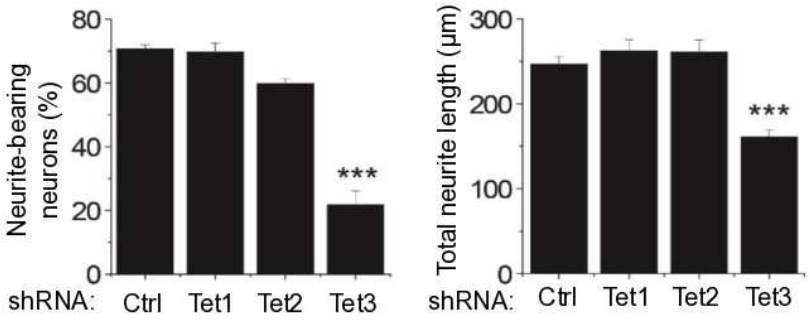

FIGURE 3.28. in vitro culture of DRG neurons: *Sample image of neurite outgrowth assay (scale bar: 100 µm).*

FIGURE 3.29. Quantification of in vitro culture of DRG neurons: *Quantification of percentages of neurite bearing neurons and total neurite length. Values represent mean ± SEM (n = 3 independent experiments; ***P < 0.001; two-way ANOVA).*

Figure 3.30

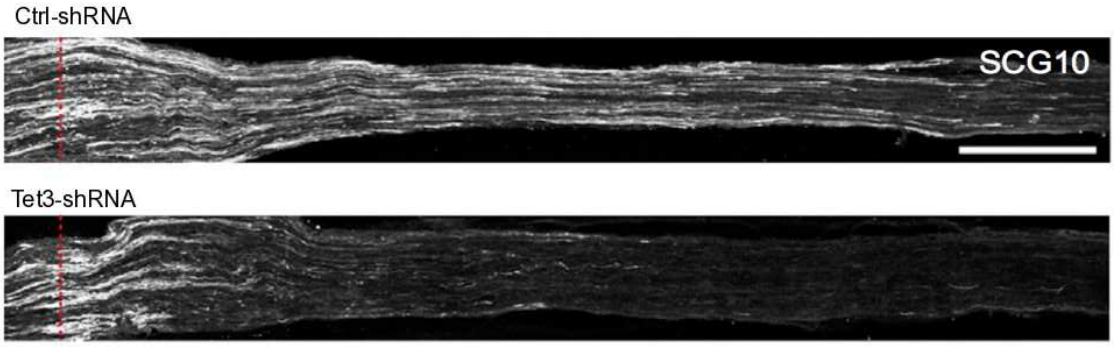

Figure 3.31

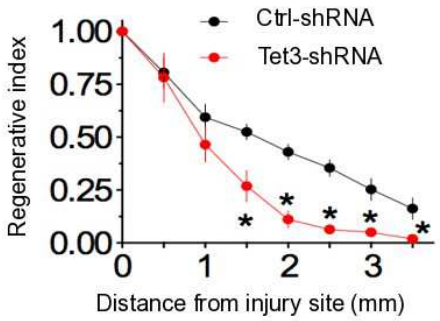

FIGURE 3.30. Tet3 KD IHC sciatic nerve regeneration, longitudinal: *Analysis of regeneration of sensory axons by SCG10 immunostaining at SNL D3. Shown are sample images of regenerating sensory axons identified by SCG10 (scale bar, 500 mm) and quantification*

FIGURE 3.31. Tet3 KD longitudinal sciatic nerve quantification: *SCG10 immunofluorescence intensity was measured at different distal distances and normalized to that at the lesion site as the regenerative index. Values represent mean ± SEM (n = 5 for each group; *p < 0.05; two-way ANOVA).*

Figure 3.32

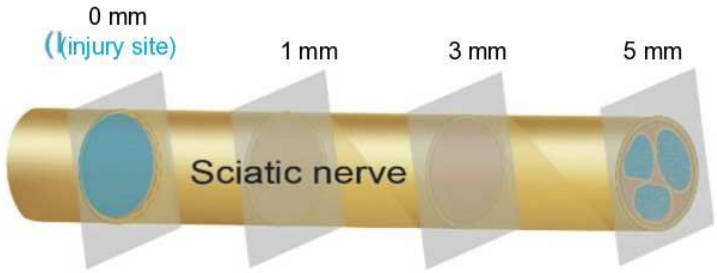

Figure 3.33

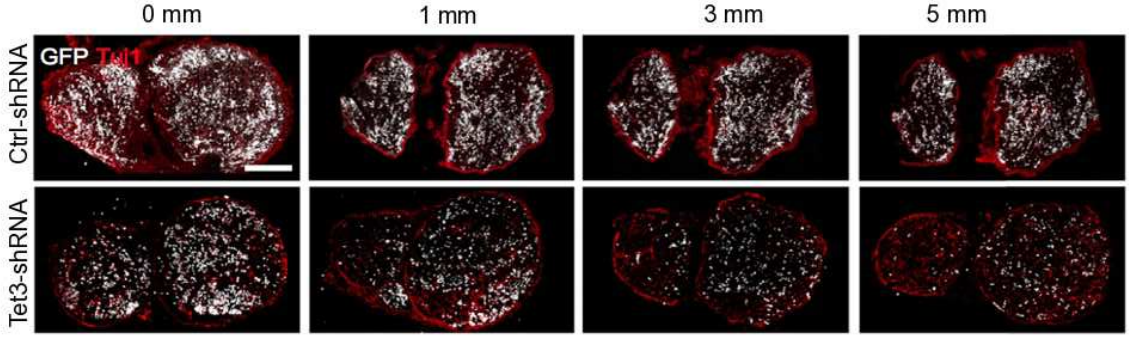

FIGURE 3.32. Sciatic nerve coronal sectioning schematic: *A schematic diagram of quantification of regenerating axons in the sciatic nerve at distal distances from the injury site (set as 0 mm).*

FIGURE 3.33. Tet3 KD IHC sciatic nerve regeneration, coronal: *Analysis of regenerating axons visualized by GFP labeling at SNL D7. Cross-sections of sciatic nerves at 1 to 6 mm distal to the lesion site from AAV-Ctrl and AAV-Tet3 KD treated animals were analyzed. Shown are sample images of GFP and Tuj1 (scale bar, 300 mm).*

Figure 3.34

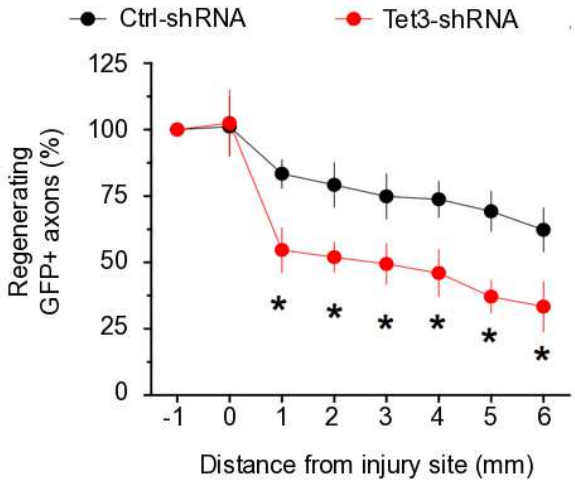

Figure 3.35

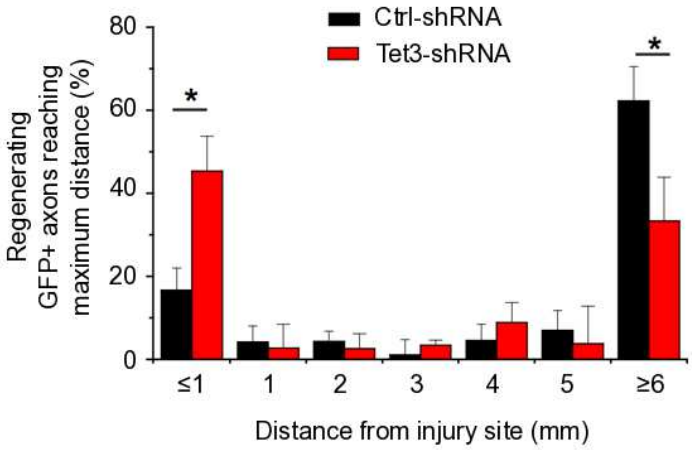

FIGURE 3.34 & FIGURE 3.35. Tet3 KD coronal sciatic nerve quantification: *Quantification of coronal sections. Values represent mean ± SEM (n = 3–4 for each group; *p < 0.05; two-way ANOVA).*

.

Figure 3.36

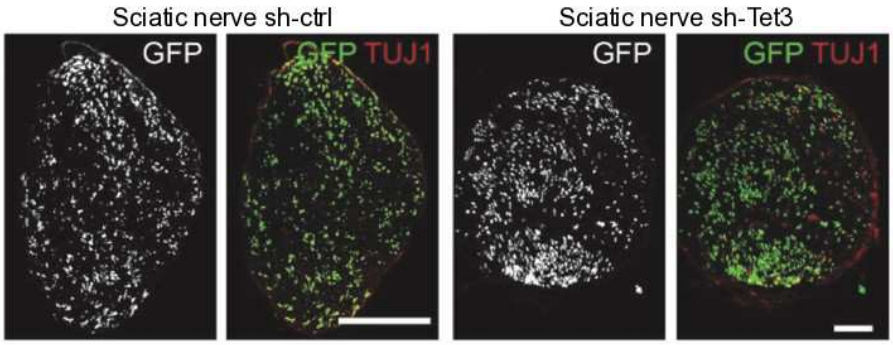

Figure 3.37

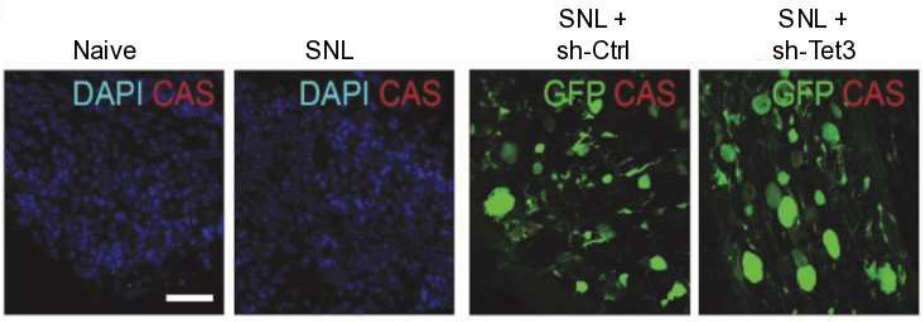

FIGURE 3.36. AAV efficacy: *Shown are sample images of cross sections of sciatic nerve at three weeks after AAV2/9 injection which expresses GFP together with either control shRNA or Tet3 shRNA in the absence of SNL (Scale bars: 50 μm).*

FIGURE 3.37. Caspase-3 IHC: *Immunostaining of cleaved caspase 3 (CAS) showed little death of DRG neurons under different conditions (scale bar: 50 μm).*

Figure 3.38

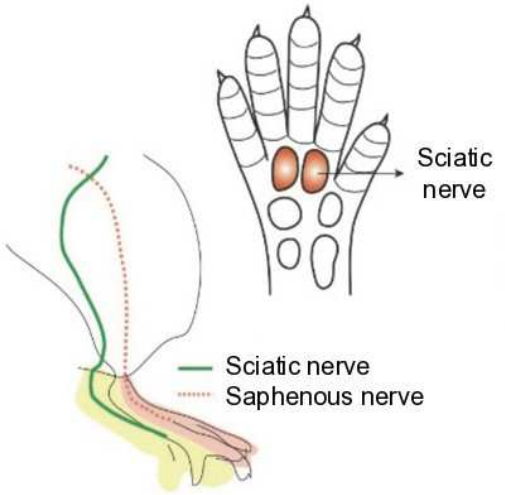

Figure 3.39

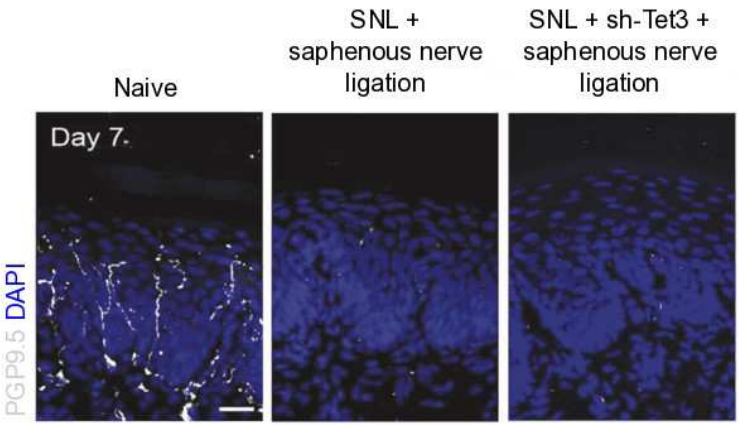

FIGURE 3.38. Skin biopsy schematic: *Schematic diagrams of skin re-innervation assay. Shown is a schematic illustration is a diagram of foot innervation illustrating the major innervation of mouse hind paw by both sciatic and saphenous nerves and the glabrous footpad regions for skin biopsy.*

FIGURE 3.39. Nerve fiber IHC, naive and D7: *Sample images of skin nerve fibers from naive and Tet3 and ctrl-shRNA animals at D7 after SNL and saphenous nerve ligation. Note that there is complete denervation of GFP+ axons in the footpad skin at D7 after injury for both control and Tet3 KD animals. Scale bar: 20 μm.*

Figure 3.40

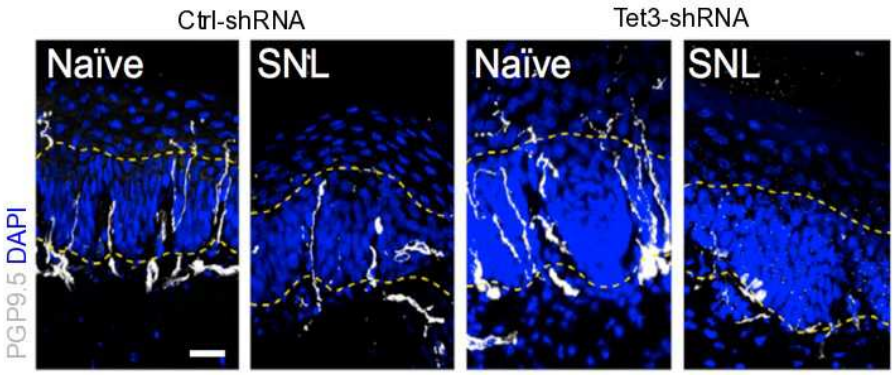

Figure 3.41

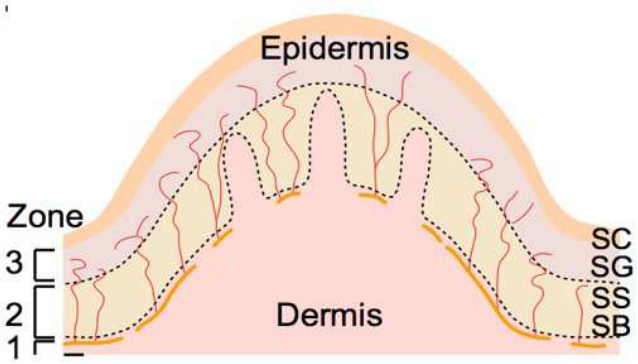

FIGURE 3.40. Nerve fiber IHC, D21: *Assay of re-innervation of epidermal area of the hindpaw by regenerating sensory axons. Shown are sample images of cross sections of hindpaw glabrous skin of Ctrl and Tet3 KD mice immunostained with the pan neuronal marker PGP9.5. The dotted line indicates the border between dermis and epidermis (Scale bar, 20 mm).*

FIGURE 3.41. Skin biopsy quantification schematic: *Shown is a schematic diagram zones we designated for quantification.*

Figure 3.42

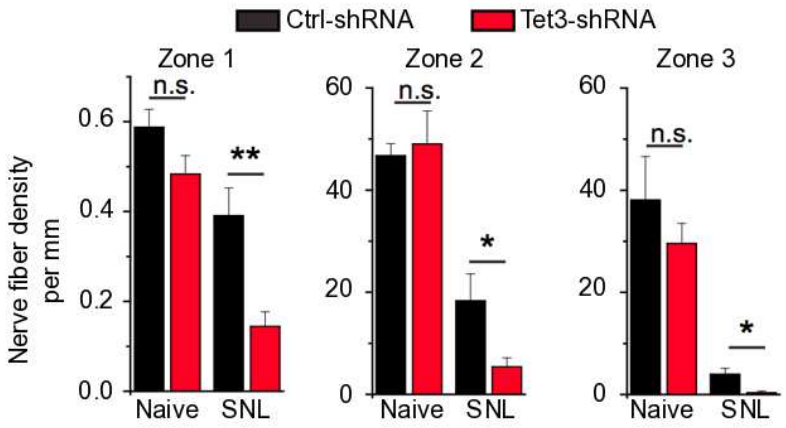

Figure 3.43

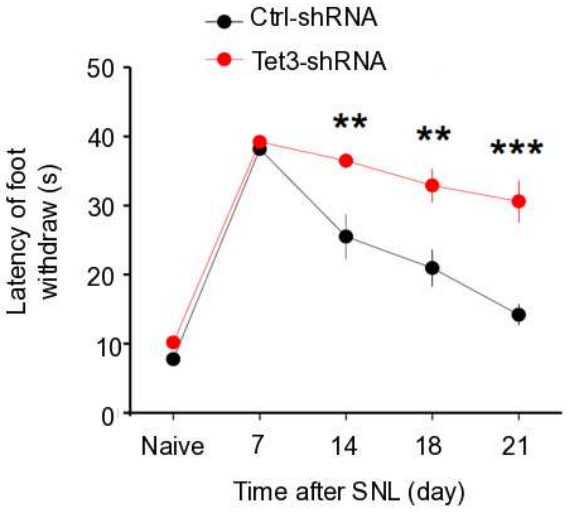

FIGURE 3.42 Skin biopsy quantification: *Quantifications of the number of intraepidermal nerve fibers in a 1 mm segment of different epidermal areas. Values represent mean ± SEM (n = 4 for each group; **p < 0.01; *p < 0.05; n.s. p > 0.1; two-way ANOVA).*

FIGURE 3.43. Thermal hindpaw withdrawal assay: *Assessment of thermal sensory recovery after SNL in AAV-Ctrl and AAV-Tet3 KD treated animals. Values represent mean ± SEM (n = 9–12 animals per group; **p < 0.01; ***p < 0.001; two-way ANOVA).*

Figure 3.44

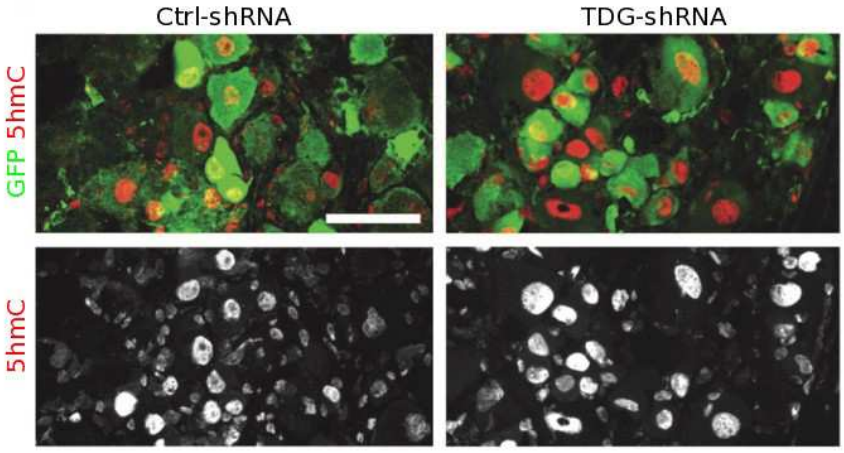

Figure 3.45

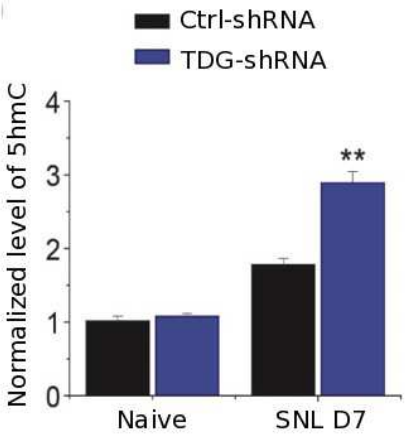

FIGURE 3.44. 5hmC IHC in TDG KD: *Immunohistochemical analysis of 5hmC levels in Ctrl and TDG KO DRG neurons of naïve and SNL D7 animals. Same as in Figure 3.14 (scale bar, 20 mm).*

FIGURE 3.45. Quantification of 5hmC IHC in TDG KD: *Quantification of TDG-shRNA 5hmC levels. Values represent mean ± SEM (n = 3; **P < 0.01; two-way ANOVA).*

Figure 3.46

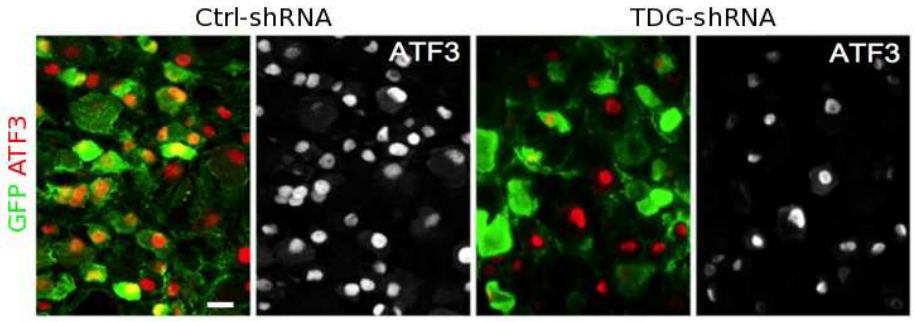

Figure 3.47

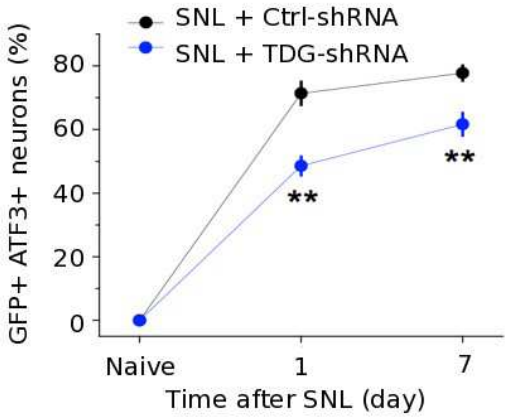

FIGURE 3.46. ATF3 IHC in TDG KD: *Assessment of ATF3 induction in TDG KO DRGs. Similar to Figure 3.18, shown are sample images (scale bar, 20 mm).*

FIGURE 3.47. Quantification of ATF3 IHC in TDG KD: *Quantification of ATF3 time course in TDG and ctrl-shRNA. Values represent mean ± SEM (n = 4 for each group; **p < 0.01; two-way ANOVA).*

Figure 3.48

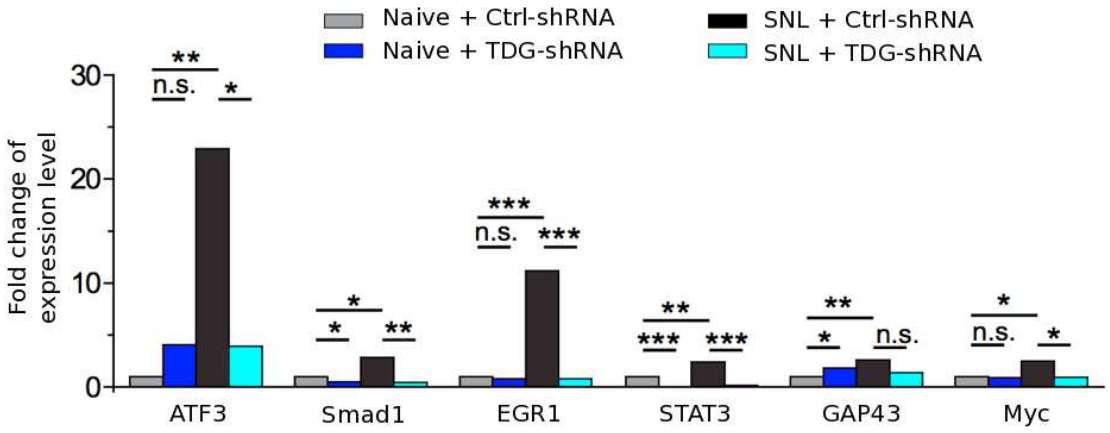

FIGURE 3.48. qPCR of RAG expression in TDG and ctrl-shRNA: *TDG-dependent expression of multiple SNL- induced RAGs. The mRNA expression was assessed by qPCR at SNL D1 and compared to the Ctrl naive group. Values represent mean ± SEM (n = 3 for each group; ***p < 0.001; **p < 0.01; *p < 0.05; n.s. p > 0.1; two-way ANOVA).*

Figure 3.49

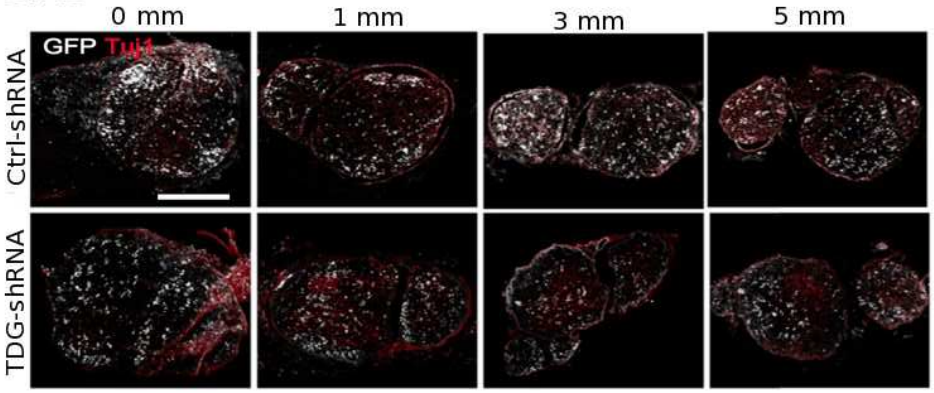

Figure 3.50

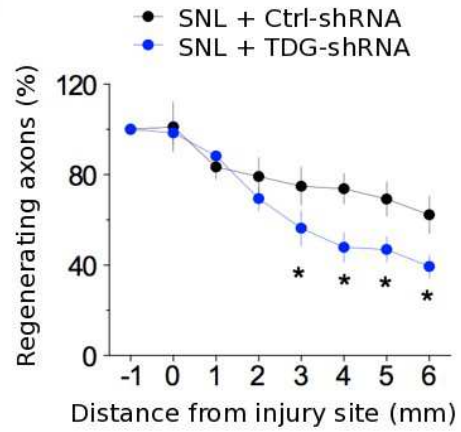

FIGURE 3.49. TDG KD IHC sciatic nerve regeneration, coronal: *In vivo axon regeneration assay. Similar to Figures 3.33. Shown are sample images (scale bar, 300 mm) at SNL D7 with expression of control-shRNA or TDG-shRNA.*

FIGURE 3.50. TDG KD coronal sciatic nerve quantification: *Quantification of coronal sections. The same data from Ctrl-shRNA in Figure 3.34 is replotted for comparison. Values represent mean ± SEM (n = 4 for each group; *p < 0.05; two-way ANOVA).*

Figure 3.51

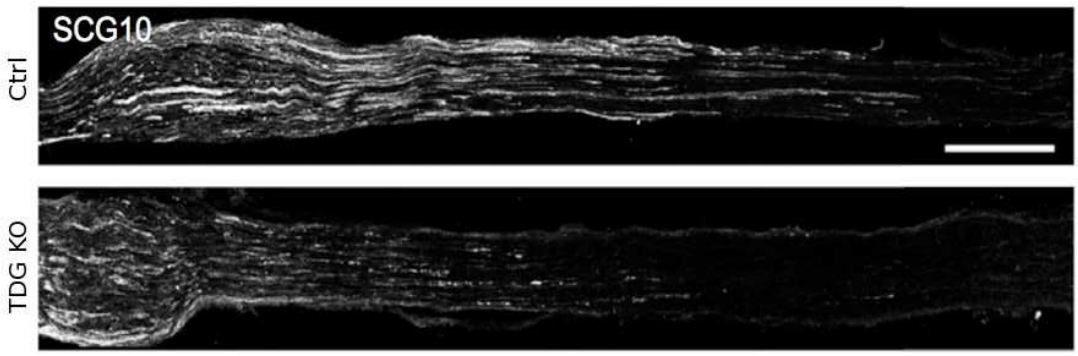

Figure 3.52

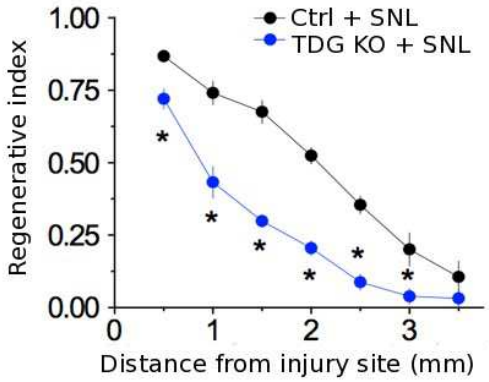

FIGURE 3.51. TDG KO IHC sciatic nerve regeneration, longitudinal: *Similar to Figures 3.30 and Figure 3.31. Shown are sample images of regenerating sensory axons identified by SCG10 (scale bar, 500 mm) in TDG$^{f/f}$ mice expressing GFP (Ctrl), or GFP and Cre (TDG-KO) and quantifications*

FIGURE 3.52. TDG KO longitudinal sciatic nerve quantification: *Quantification of regeneration in TDG KO. Values represent mean ± SEM (n = 4 for each group; *p < 0.05; two-way ANOVA).*

Figure 3.53

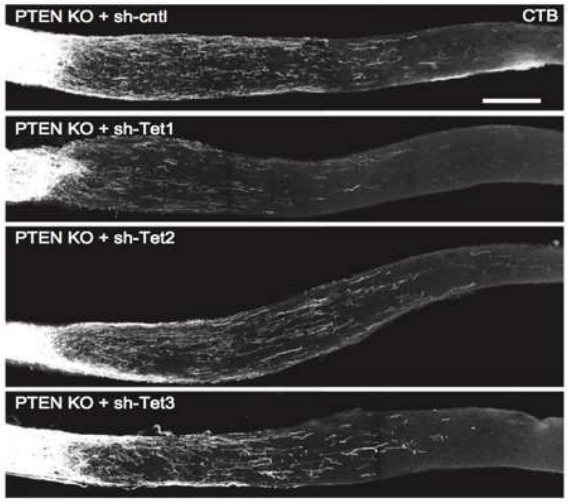

Figure 3.54

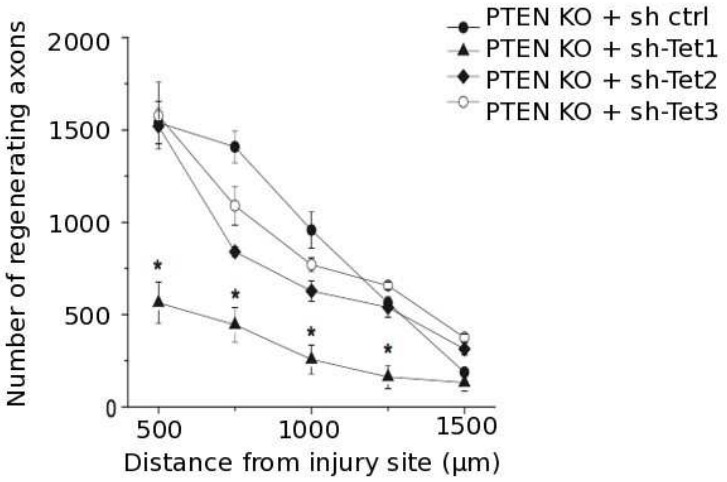

FIGURE 3.53. PTEN/Tet KD IHC: *Adult Pten$^{f/f}$ mice were injected with AAVs to co-express GFP, Cre, and control shRNA, or shRNA against Tet1, Tet2, or Tet3, followed by optic nerve crush 2 weeks later. RGC axons were anterogradely labeled by cholera toxin b subunit 12 days after injury. Shown are sample images of labeled axons (scale bar, 20 mm).*

FIGURE 3.54. PTEN/Tet KD quantification*: Quantification of PTEN KO optic nerve regeneration. Values represent mean ± SEM (n = 3 for each group; *p < 0.05; two-way ANOVA).*

CHAPTER 4 - DISCUSSION

In the PNS, mature, post-mitotic neurons are able to activate a pro-regenerative program that not only produces axon regrowth and proper axon targeting, but can fully restore the functionality of injured neurons [1, 112]. Together with extrinsic factors, the intrinsic system is an important component of regeneration [3, 113]. In this study, we have identified a critical component of the intrinsic pro-regenerative program that is essential for PNS regeneration, DNA demethylation. Together with histone modifications, DNA methylation regulates intrinsic regeneration capacity [78]. In addition to offering insight into the basic biology of regeneration, this new data suggests novel therapeutic targets for both PNS and CNS regeneration.

4.1 Current models of CNS regeneration

The existing methods to increase regeneration in the CNS show surprising potential. For example, the PTEN KO described above has been further improved and refined by synergistically combining other regulatory elements, such as the PTEN/SOCS3 double KO [111, 114, 115]. However, PTEN is an oncogene, and therefore, not ideally suited to be a therapeutic target [116, 117]. Our work with PTEN suggests that there is an epigenetic component to the observed regeneration phenotype (Figure 3.53, 3.54). With further development, one potential application is the upregulation of pro-regenerative regulatory elements such as Tets or HATs (Figure 3.53) [78]. Still, much further research is necessary to understand how these elements function in their native system.

4.2 Tet1 Overexpression

Our data suggest that Tet1 is essential for PTEN-related regeneration gains in the CNS (Figure 3.53). However, additional experiments in our lab using the overexpression of Tet1 were unsuccessful in increasing CNS regeneration. Although PTEN KO-associated regeneration requires Tet1, Tet1 overexpression alone is not sufficient to cause an increase in regeneration. There are likely many reasons for this. First, when the peripheral nervous system upregulates Tet3, it also targets it to the correct methylated loci. Our data show that Tet3 does not bind every methylated enhancer, even those within essential RAGs, such as Gap43 (Figure 2.17, 2.26). Thus, the simple upregulation of single regulatory factors is unlikely to be successful. One future direction of this work, as well as the wider epigenetic field, is to better understand how epigenetic regulators find their correct targets. A second possible reason Tet1 upregulation is unsuccessful as an independent therapeutic target is the role of translation. Although this work has focused on the role of transcription in regeneration, translation is also an essential component of the wider intrinsic regenerative program. Large amounts of newly-synthesized protein are required to successfully repair and extend injured axons [118].

4.3 m^6A and regeneration

One way that the PTEN KO model successfully induces regeneration is by activating the mTOR pathway [111]. In the PNS, the mTOR pathway is active both

under basal conditions and after injury [96, 119]. However, in the CNS, mTOR signaling declines as the neuron matures, and is completely blocked upon CNS injury [96].

mTOR is a regulator of cap-dependent translation [120]. Based on the connection between PTEN and cap-dependent translation, a new direction in our lab has focused on the role of the epitranscriptome in the regulation of translation efficiency after SNL. The epitranscriptome is comprised of a diverse group of chemical modifications on RNA, and associated RNA binding proteins, which dynamically regulates the fate of RNA. To date, many modifications have been discovered, including N^6-methyladenosine (m^6A), N^1-methyladenosine (m^1A), and 5-methylcytosine (m^5C) [121-124]. Of these modifications, m^6A is the most abundant, and, together with its binding partners, has been show to increase translation [125, 126]. An ongoing project in our lab focuses on the role of m^6A in PNS regeneration. Our data suggests that m^6A is a regulator of protein translation following SNL. Therefore, m^6A opens a new avenue in regeneration, protein translation regulation and the epigenome.

Like Tet1 OE, modulation of m^6A is also unlikely to independently promote proper regeneration in the PNS. It has been suggested that mTOR is dispensable for axonal regeneration in the PNS because rapamycin, a specific mTOR inhibitor, does not suppress the axon growth in the DRG [38, 127]. Indeed, even with an increase in translation, the PNS still requires proper *de novo* transcription of

epigenetically silenced RAGs. Therefore, true gains in therapeutic CNS regeneration are likely to involve a regulated system of transcription and translation. Further, any model must work within the context of the individual cell targeted.

4.4 Other methods of CNS regeneration

Although great gains have been made by applying PNS regeneration factors to the CNS, the CNS itself has also yielded important data. For example, a small injury in the CNS which occurs before a large injury preconditions the CNS to respond more favorably. This preconditioning not only prevents neurons from undergoing apoptosis, but can lead to gains in regeneration [128, 129]. As the conditioning lesion must be delivered before the injury, the method is of little therapeutic consequence. However, understanding what factors are upregulated in the CNS as a result of the conditioning lesion has provided valuable insight into CNS regeneration. For example, cAMP injection appears to approximate the regenerative program of the preconditioned CNS [130-133]. Combing the insights learned from the PNS with the preconditioning CNS model might be a good way to better understand the intricacies of CNS regeneration. As an illustration, we discovered the role of Tet3 in regeneration using the PNS as a model system. In the PTEN KO model, Tet1 was implicated, but the use of Tet1 overexpression alone was insufficient to cause CNS regeneration. Now that the role of DNA demethylation in PNS regeneration has been illuminated, the role of Tet can be directly investigated in the CNS using a model such as the preconditioning system.

4.5 CNS development and regeneration

The fetal CNS offers another model for CNS regeneration. During development of the nervous system, regeneration is robust and precise after injury [70]. As discussed above, neurons proceed down a developmental path that silences fetal gene expression and activates those genes essential for the mature neuron [59]. In the CNS, neurons are competent to regenerate until just after birth in mice [70]. This signaled loss of regenerative capacity is mediated by cellular transduction [70]. Neurons that do not receive the signal to turn off axon growth persist in their regenerative ability. Further, neurons that receive the signal and switch to dendritic growth, retain this state even if the signal is removed [70]. Therefore, it is probable that epigenetic factors program the neuron's switch from an axon growth state to an adult, non-regenerative state. Preliminary data in our lab suggests that several epigenetic modifiers are upregulated at the time of the transition from axonal to dendritic growth. Once mature CNS neurons have reached their target, they are unable to reform a growth cone or synthesize the cytoskeletal elements necessary for axon elongation [134]. Therefore, if the CNS neuron could be returned to its embryonic growth state, for instance through modulation of epigenetic factors, the cell could be induced to regenerate as it does before reaching maturity. This, however, comes with two major caveats. First, there is no guarantee that the regenerative program matches embryonic development. Indeed, the PNS clearly has a special program for regeneration. Second, there are many signals, from

many different cells, that give guidance and growth cues to the developing neuron. Clearly, regeneration will require proper orchestration of a large variety of cells.

4.6 Preconditioning and adult neurogenesis

There are also two innate ways that adult CNS neurons can produce new growth. First, specific centers of the brain can produce fully functional new neurons from existing adult precursors in a process known as adult neurogenesis [135, 136]. Because these cells develop in the brain without manipulation, they integrate into the existing neural network seamlessly. Therefore, these newborn neurons could be useful as a system-wide approach to understanding how regenerative CNS growth could be acclimatized. The two major regions of neurogenesis in mammals are the olfactory bulb and the dentate gyrus of the hippocampus [137, 138]. Second, it has been suggested that there are other, non-neurogenic zones in which reactive astrocytes, a major hallmark of CNS injury, might be reprogrammed to form new neural progenitor cells [139-141]. This suggests that, despite the extrinsic limitations of the CNS, intrinsic programs can allow for axon extension.

Together, the data on CNS growth, axon extension, and regeneration reveals a dynamic, tightly regulated system. Although CNS neurons are mature and post-mitotic, it is possible that functional connections can be made after injury. However, the CNS, like the PNS, is a heterogeneous system. Therefore, therapeutic approaches will likely need to be discrete and specific. It is possible that each individual cell of the nervous system will require its own pro-regenerative system.

4.7 Applications to the PNS

Due to of the huge burden of morbidity and mortality in CNS disease, it is necessarily a major focus of regenerative research [2]. However, the PNS also presents regeneration hurdles. As an organism ages, the PNS gradually loses its ability to regenerate [142-144]. In rodents, the number and speed of regenerating axons is greatly reduced with age [143, 145]. In addition, neurodegeneration is a critical problem amongst many common diseases, including Parkinson's and diabetes [146]. Gains in PNS regeneration will also be of great benefit to PNS disease.

4.8 Other epigenetic factors

This work, together with previous studies, has identified the role of epigenetic modifications in PNS regeneration. A current study in the lab is expounding on the role of m^6A, an RNA modification. However, there are still many more regulatory epigenetic elements that have not yet been investigated. For example, m^6A is only one of a number of RNA modifications that have been shown to effect translation and stability of RNA molecules [124]. There are still many other epitranscriptomic modifications that have not yet been investigated. Further, the organization of genome under PNS injury is still unexplored. Methods such as ATAC-seq have shown large genomic changes with neuronal activity in the CNS [76, 147]. Alteration of the chromatin landscape changes accessibility of the DNA to a wide variety of proteins, such as transcription factors and the transcription machinery, thereby altering genomic expression. In addition, recent mapping of the 3D

structure of the genome has yielded insight into genomic neighborhoods that function together, insulated from nearby neighborhoods [148, 149]. Although the upregulation of many RAGs was explained by Tet3, some, such as GAP43, were not demethylated, and are, therefore, regulated by a different method, possibly through chromatin architecture (Figure 3.22, 3.23).

4.9 Soma and axon growth

The molecular data in this work was collected exclusively in the soma. As the center of transcription, the soma provides the essential blueprint for regeneration. However, the ends of the regenerating axons are also extremely active. These distal regions must coordinate the work of rebuilding an axon. For example, because of the extensive distance between the soma and growth cone, many mRNAs are transported from the soma, and protein synthesis occurs on site [150-152]. Although technical limitations make studying RNA molecules in the axons difficult, recent advancements are allowing interrogation of this system [153]. A better understanding of which mRNAs are transported to the axons ends and how this regulatory system functions will add greatly to the knowledge of how PNS regeneration occurs. Future work in this area should address the role of RNA modifications, m^6A and others, in the packaging and transport of mRNAs, as well as the regulation of translation at the axon ends.

4.10 Conclusion

This work has focused on a small but essential component of regeneration: regulation of intrinsic RAG expression. We found that Tet3 is upregulated through retrograde signaling, in turn demethylating and upregulating RAGs. Adult neurons regulate the expression of these genes though the combined activity of epigenetic factors. In the PNS, these regulatory elements can be reprogramed within the adult cell to allow for functional regeneration. Although there is still much to be explored, this work provides a novel, important advancement to the field of regeneration.

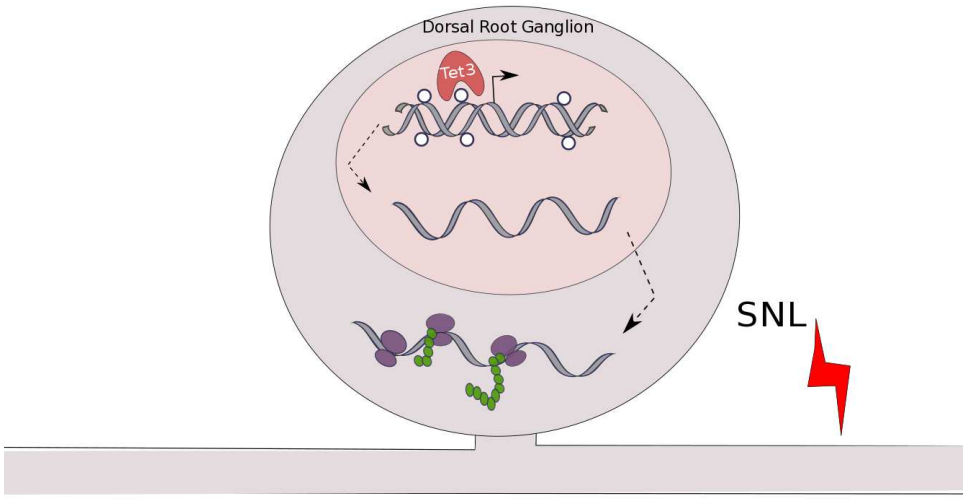

FIGURE 4.1. Graphical abstract of thesis: *SNL upregulates Tet3 in the dorsal root ganglion. Tet3 is recruited to and demethylates regions of specific, key RAGs, allowing their expression. The upregulation of transcription is a key component of the intrinsic regeneration program in the PNS.*

CHAPTER 5 - METHODS

5.1 AAV constructs

Ctrl shRNA and shRNAs for mouse Tet1, Tet2, and Tet3 were previously characterized [88, 154]. Tet3 shRNA efficacy was further validated by qPCR in DRG neurons both *in vitro* and *in vivo* (Figure 5.1). shRNA for mouse TDG contained the following short-hairpin sequence: AAATGTCAGGAAGAGTCTTGG and its efficacy was validated by qPCR in the DRG *in vivo* (Figure 5.2). High titers of recombinant AAV2/9 virus transducing shRNA were generated as previously described [154, 155]. In addition, the recombinant AAV2/9 vector for Cre was purchased from the UPenn Vector Core.

5.2 DRG cultures and neurite outgrowth assay

For cell culture experiments, lumbar DRGs from adult mice were rapidly dissected and digested in a solution of Collagenase II (200 U/mL, Worthington Biochemical Corporation, Lakewood, NJ) and Dispase II (2.5 U/mL, Roche Diagnostics) in HBSS at 37 C for 30 min. Tissues were then mechanically dissociated into cell suspension by gentle trituration with a 1 mL pipette tip. The cell suspension was layered on a BSA cushion (10% w/v in F12/MEM) and centrifuged at 600 g for 15 min to remove myelin and axon debris. Purified neurons were then cultured on laminin-coated coverslips in F12/MEM media complemented with 10% FBS and penicillin-streptomycin at 37 C. Cultures were infected with AAV co-expressing GFP and different shRNAs for 5 days. Cultures were then trypsinized (0.025% Trypsin-EDTA) for 5 min at 37 C, gently triturated in fresh medium with 10% FCS,

and cultured for additional 16 hr. Cells were fixed with 4% PFA and neurites were visualized by immunostaining of β-tubulin (Tuj1; Sigma, 1:1000). The percentage of neurons bearing neurites was quantified by counting those with neurites longer than the diameter of its soma. The length of the longest neurite in each cell was measured in neurite-bearing neurons using the NeuronJ software. Approximately 150 cells were scored per condition and three independent sets of experiments were performed.

For the pharmacological experiments, lumbar vertebrae were rapidly dissected and treated with BAPTA-AM (50 mM), KN92 or KN93 (10 mM) in DMEM/F12 media for 1 hr at 37 C in a humidified atmosphere containing 5% CO2. Total RNA was then isolated from the DRG using TRIzol and RNA Clean and Concentrator (Zymo Research) for the subsequent qPCR assay.

5.3 Animal surgery

For intrathecal injection of AAV2/9 virus, adult mice were anesthetized and shaved to expose the skin around the lumbar region. A total of 3 mL of viral solution was injected to cerebrospinal fluid between vertebrae L5 and L6 using a 30 gauge Hamilton syringe. The injection needle was left in place an additional 2 min to allow the fluid to diffuse. Mice were left to recover for 3 weeks to ensure substantial viral expression prior to behavioral or surgical procedures.

For the SNL surgery, mice were anesthetized and a small incision was made on the skin at the mid-thigh level. The sciatic nerve was exposed after opening the fascial plane between the gluteus superficialis and biceps femoris muscles. The nerve was carefully freed from sur- rounding connective tissue and then crushed for 15 s at 3 clicks of ultra-fine hemostatic forceps (F.S.T. 13021-12). The crush site was labeled by stitching a 10-0 nylon suture through the epineurium. The skin was then closed with two suture clips. For the sham (naive) surgery, the sciatic nerve of the contralateral side was exposed and mobilized but left uninjured. For the thermal withdrawal test and skin biopsy experiments, the saphenous nerve was ligated and transected above the knee region after sciatic nerve crush, so that the hind paw epidermis can only be innervated by regenerating sciatic nerve axons.

5.4 Behavioral analysis

The thermal withdrawal behavioral test was performed following a previously established protocol [102]. Briefly, mice were placed on a glass surface with a consistent temperature of 30 C. The plantar surface of hind paw was tested using a focused, radiant heat light source (model 33 Analgesia Meter; IITC/Life Science Instruments, Woodland Hills, CA, USA). A timer linked to the light source was used to measure the paw-withdrawal latency. Only quick hind paw movements away from the stimulus were considered to be a withdrawal response, and seven individual measurements were repeated for each paw.

5.5 In situ hybridization

In situ hybridization was performed on PFA-fixed DRG sections (20 mm thickness) as described previously [74, 156]. Digoxigenin-labeled antisense riboprobes specific for the coding sequences of mouse Tet1 (3353-3860 bp), Tet2 (2808-3366 bp) and Tet3 (4977-5616 bp) were generated using the DIG RNA labeling kit (Roche Applied Science) according to the manufacturer's instructions. DRG sections were hybridized with riboprobes at 60 C overnight, and then washed once in 5X SSC and three times in 0.2X SSC for 30 min each at 60 C. DRG sections were incubated with alkaline phosphatase-conjugated anti-digoxygenin antibody at 4 C overnight and developed in nitroblue tetrazolium (NBT, 35 mg/ml)/5-bromo-4-chloro-3-indolyl phosphate (BCIP, 18 mg/ml) solution at room temperature to visualize hybridized riboprobes. Experiments for different conditions were processed in parallel for comparison. For the combined immunocytochemistry and fluorescence *in situ*, the same *in situ* procedure was followed as above with the following exceptions. First, an RNA probe was generated and conjugated to alexa fluor 594 (FISH Tag #F32954). Second, *in situ* hybridization was followed by immunostaining for GFP (goat anti-GFP Rockland; 1:500), incubated at 4 C overnight and followed by a two-hour room temperature incubation of cy2-conjugated secondary (Jackson ImmunoResearch; 1:500).

5.6 Western blot analysis

L4/L5 injured or naive DRGs were rapidly dissected and extracted protein samples were run on 4%–16% Mini-PROTEAN TGX Pre- cast Protein Gels (Bio-rad) and

transferred to PVDF membrane using the transblot turbo system (Biorad) following manufacturer's instructions. The membrane was blocked overnight in 5% dry milk at 4 C with rocking. Anti-Tet3 antibodies (Abiocode; 1:1000) were applied overnight at 4 C followed by HRP-conjugated mouse anti-mouse IgG antibody (Santa Cruz; 1:4000). Protein loading was verified by mouse anti-GAPDH.

5.7 Gene expression and methylation analyses

For qPCR analysis, L4 and L5 DRGs were rapidly dissected from adult mice and homogenized with Trizol (invitrogen) to extract total RNA. Isolated RNA was reverse transcribed to cDNA (Invitrogen) and the expression level of target genes was measured by qPCR with Fast SYBR Green Master Mix (ABI). Specific primers used in this study are listed in Table 1.

A restriction enzyme-based methylation assay was performed to quantify levels of DNA methylation at select loci in mouse DRG DNA as previously described [50, 157]. Briefly, 500 ng of genomic DNA from neuronal nuclei enriched by a sucrose cushion method were digested with MspI, HpaII or mock for 8 hr at 37 C. The reaction was stopped by treatment of proteinase K for 10 min at 40 C and heat-inactivation for 5 min at 95 C. DNA samples were then diluted with ddH2O to 150 mL final volume and were assayed by Q-PCR (Applied Biosystems 7500) using Power SYBR Green PCR Master Mix (Applied Biosystems). Primers flanking specific HpaII digestion sites (CCGG) are listed in Table 2.

5.8 In vivo DRG axon regeneration assay

Adult mice were anaesthetized and perfused with 4% PFA in PBS. For cross-section analyses, the sciatic nerve was harvested at 7 days-post crush when degeneration of preexisting axons of mature neurons was complete (Di Maio et al., 2011; Shin et al., 2012). DRGs were dissected and post-fixed in fixative at 4 C for 5 min. The sciatic nerve was post-fixed overnight, and the cryoprotected in 30% sucrose (wt/vol) for 24 hr at 4 C. The nerve was sectioned into 10 mm thickness at every 1 mm, from 1 mm proximal to injury site (-1) to 6 mm distal to injury site. The sectioned nerves were stained with anti-GFP antibody and the total number of axons was quantified at each distance by using ImageJ software. The section (-1) proximal to injury site served as control and the axon number in other sections was normalized to the control for each animal to assess the regeneration rate.

For the longitudinal sections assay, sciatic nerves were dissected at SNL D3 and postfixed with 4% PFA. Longitudinal sections were stained with SCG10 (Novus Biologicals, NBP1-49461). SCG10 fluorescence intensity was measured by NIH ImageJ along the distance as previously described [100, 158]. An SCG10 intensity plot was drawn with average intensities calculated from non-overlapping 10 mm regions and normalized to that observed at the crush site.

5.9 Immunohistochemistry

IHC was performed as described previously [159]. The slides were incubated with primary antibodies at 4 C overnight. Primary antibodies used in this study include:

mouse anti-Tuj1 (Sigma; 1:1000 or BioLegend; 1:2000), mouse anti-phospho-c-Jun (Cell Signaling; 1:300), rabbit anti-5hmC (Active Motif; 1:5000), rabbit anti-ATF3 (Santa Cruz; 1:500), rabbit anti-PGP9.5 (AbD Serotec; 1:800), goat anti-GFP (Rockland; 1:500), mouse Anti-NeuN (Millipore; 1:500), mouse anti-Glutamine Synthetase (Santa Cruz sc-74430; 1:300), rabbit anti-SCG10 (Novus Biologicals, NBP1-49461, 1: 2000), and anti-cleaved (active) form of caspase 3 (Invitrogen, 9H19L2; 1:500). Cy2–, Cy3– or Cy5–conjugated secondary antibodies (Jackson ImmunoResearch; 1:500) to appropriate species were incubated at room temperature for 2 hr. The images were acquired by confocal microscopy (Zeiss 710).

Images were analyzed with ImageJ software (National Institutes of Health). Quantification of the proportion of ATF3 or p-c-Jun ex- pressing DRG neurons was determined by counting the number of immunoreactive (with nuclear signal) and non-immunoreactive (without nuclear signal) neurons. The cutoff value for determining the threshold of immunoreactivity was based on the negative cells in naive samples processed in parallel. All cells with fluorescence signal above threshold were considered positive. At least 50 GFP+ DRG neurons per mouse were counted on randomly chosen sections from L4 and L5 DRGs.

For skin biopsies, glabrous footpad skin from hind paws was harvested by punch biopsy. The biopsy was immersion-fixed in Zamboni's fixative overnight at 4 C, and cryoprotected in 30% sucrose. The specimens were then sectioned at 20 mm,

mounted on gelatin coated slides and stained with rabbit anti-PGP9.5 antibody to visualize nerve fibers. To quantify regenerative nerve fibers, we defined 3 zones based on the structure of skin. Zone 1 is the dermis layer where the subepidermal nerve plexus length (SNPL) was determined and divided by the length of epidermis. Zone 2 and Zone 3 are defined based on the boundary between stratum granulosum (SG) and stratum spinosum (SS) sub-layers in epidermis. The density of epidermal nerve fibers was measured by counting numbers of nerve fibers per mm of epidermis. Nerve fibers branching within Zone 3 were counted as one, whereas nerve fibers branching within Zone 2 were counted separately.

5.10 Neuronal nuclei isolation

For 5hmC quantification, we enriched DRG neurons with a sucrose cushion method [160]. Briefly, frozen DRG tissues were ground into fine powder in a dry ice/ethanol cooling bath and homogenized in 3 mL of hypotonic buffer containing 20 mM Tris-HCl (pH 7.4), 10 mM NaCl, and 3 mM MgCl2. Samples were then suspended in nuclei resuspension buffer containing 3 mM MgCl2, 5 mM CaCl2, 10 mM Tris-HCl (pH7.5), 0.5 mM DTT, 1x proteinase inhibitor (Roche), and 0.32 M sucrose. The crude nuclei were layered onto a sucrose cushion buffer containing 0.5 mM MgCl2, 0.5 mM DTT, 1x proteinase inhibitor, and 0.88 M sucrose, and centrifuged at 2800 g for 15 min at 4 C to enrich the neuronal nuclei population. The neuronal nuclei were then resuspended in nuclei resuspension buffer for cytometry analysis or methylation sensitive qPCR analysis.

5.11 5hmC dot blot analysis

Dot blot analysis of 5hmC was performed as previously described [88, 154]. Briefly, genomic DNA samples from different treatment groups were adjusted to a concentration of 100 ng/ml, heat-denatured at 95 C for 5 min, and chilled on ice for 1 min. Samples were applied to Hybond-N+ membranes (GE Healthcare), and then cross-linked by a UV stratalinker 1800 (Stratagene). Membranes were blocked by 5% dry milk (wt/vol), and incubated with anti-5hmC antibody (Active Motif; 1:5,000) followed by HRP-conjugated donkey anti-rabbit IgG antibody (Santa Cruz; 1:1000). Signal was visualized by SuperSignal West Pico Chemiluminescent Substrate (Thermoscientific).

5.12 Bisulfite sequencing

Bisulfite sequencing analysis was performed as previously described [74]. Briefly, genomic DNA was bisulfite converted using commercial reagents (Zymo Research). The converted DNA was then used as a template for PCR amplification of regions of interest with specific primers (listed in Table 3). PCR products were gel-purified and cloned into the pCR 2.1 TOPO vector (Invitrogen). Individual clones were sequenced and aligned with the reference genomic sequence.

5.13 ChIP analysis

Freshly dissected DRGs were cut into fine pieces and incubated in 1% formaldehyde (Sigma) in Dulbecco's PBS (DPBS) for 15 min at room temperature with continuous rocking. 0.125 M glycine was added to the solution and incubated

for 5 min to quench cross-links. After washing twice with ice-cold DPBS, tissue pieces were resuspended in cell lysis buffer (50 mM Tris-HCl pH 8.0, 10 mM EDTA, and 1% SDS), homogenized using a Dounce homogenizer (Kimble Chase) and then incubated on ice for 30 min. The samples were sonicated by a Bioruptor plus (Diagenode) for 25 cycles (30 s on, 30 s off) at the high intensity setting. After centrifugation, the supernatant was diluted 10 times in IP dilution buffer (0.01% SDS, 1.1% Triton X-100, 16.7 mM Tris-HCl pH 8.0, 1.2 mM EDTA, and 167 mM NaCl). Anti-Tet3 (Jin et al., 2016) or rabbit IgG (3 mg; Cell Signaling 2729) antibodies were added and incubated at 4 C over- night. Protein G Dynabeads (Life Technologies) were then added to the samples and incubated at 4 C for 2 hr. The beads were washed twice with low-salt wash buffer (0.1% SDS, 0.1% Triton X-100, 2 mM EDTA, 20 mM Tris pH 8.0, and 150 mM NaCl), twice with high-salt wash buffer (0.1% SDS, 0.1% Triton X-100, 2 mM EDTA, 20 mM Tris pH 8.0, and 500 mM NaCl), twice with IP wash buffer (1% deoxycholic acid, 1% Igepal, 100 mM Tris pH 9.0, and 500 mM LiCl) and twice with TE buffer (10 mM Tris-HCl pH8.0 and 1 mM EDTA). Freshly made elution buffer (1% SDS and 0.1 M NaHCO3, pH 8.0) was added to the beads, and chromatin was eluted at 65 C in a thermomixer for 1 hr. After removing beads, crosslinking was reversed in 0.3 M NaCl solution at 65 C overnight. Proteinase K (NEB) was then added to the decrosslinked chromatin solution and incubated for an additional 2 hr at 55 C. The eluted DNA fragments were extracted using phenol:chloroform:isoamyl alcohol (25:24:1) and precipitated by isopropanol and glycogen. Region-specific primers for Q-PCR are listed in Table 4.

5.14 Optic nerve injury and quantification

The procedure was performed as previously described [111]. Briefly, Individual AAV-shRNA for Ctrl, Tet1, Tet2, and Tet3 was mixed with AAV-Cre and intravitreally injected to the left eyes of adult PTENf/f mice. Two weeks after viral injection, the left optic nerve was exposed intraorbitally and crushed with jeweler's forceps (Dumont number 5; Roboz) for 5 s, approximately 1 mm behind the optic disc. To visualize regenerating axons, RGC axons in the optic nerve were anterogradely labeled by 1 ml of cholera toxin b subunit (CTB; 2 mg/ml; Invitrogen) 12 days after injury. Animals were fixed by 4% PFA 2 days after CTB injection in the eye. Quantification of regenerating axons was also performed according to previously described methods [111]. Specifically, for each animal the number of CTB labeled axons was estimated by counting the number of CTB-labeled fibers extending different distances from the end of the crush site in 5 sections (every 4th section) per animal. The cross-sectional width of the nerve was measured at the point at which the counts were taken and was used to calculate the number of axons/mm of nerve width. The number of axons/mm was then averaged over all sections. Σad, the total number of axons extending distance d in a nerve having a radius of r, was estimated by summing over all sections having a thickness t (8 μm): $\Sigma ad = \pi r^2 \times$ [average axons/mm]/t.

5.15 Animals

Four mouse lines were used for this study. C57Bl6/J mice, used as WT in all experiments, were purchased from Charles River. A DRG neuron reporter mouse line that expresses GCaMP3 from the endogenous Pirt locus was a gift from Xinzhong Dong [86]. The $TDG^{f/f}$ mouse line was a gift from Alfonso Bellacosa (A.B., unpublished data). The $Pten^{f/f}$ mouse line was a gift from Zhigang He [111]. Adult mice (6-8 weeks) were used.

Figure 5.1

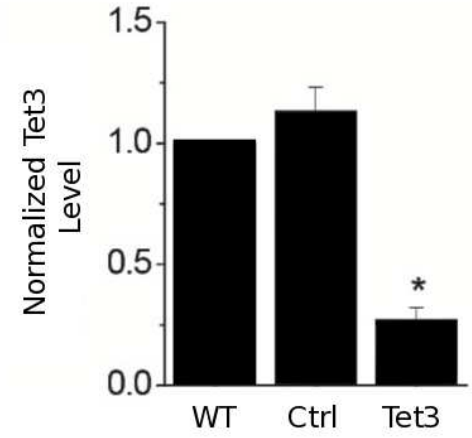

Figure 5.2

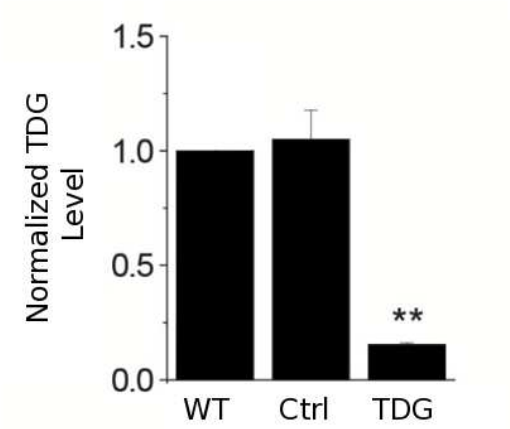

FIGURE 5.1. Quantification of Tet3 KD efficacy: *Quantification of the efficacy of Tet3 shRNA in vitro. Values represent mean ± SEM (n = 3; *P < 0.05; two-way ANOVA)*

FIGURE 5.2. Quantification of TDG KO efficacy*: In vivo knockdown efficacy of TDG shRNA. Adult DRGs were infected with AAV-TDG shRNA or ctrl- shRNA via intrathecal injection. TDG expression was analyzed 21 days later by qPCR.*

TABLE 1: qPCR primers of epigenetic regulators and RAGs

GAPDH_F	AAGAAGGTGGTGAAGCAGGCATCT
GAPDH_R	ACCCTGTTGCTGTAGCCGTATTCA
Tet1_F	GAGCCTGTTCCTCGATGTGG
Tet1_R	CAAACCCACCTGAGGCTGTT
Tet2_F	TGTTGTTGTCAGGGTGAGAATC
Tet2_R	TCTTGCTTCTGGCAAACTTACA
Tet3_F	CCGGATTGAGAAGGTCATCTAC
Tet3_R	AAGATAACAATCACGGCGTTCT
TDG_F	CCATGTAATGGGGAACCTTG
TDG_R	AAGGGATCTGCTCTGCAAAC
Gadd45a_F	TGAGCTGCTGCTACTGGAGAACGAC
Gadd45a_R	TCCTTCCATTGTGATGAATGTGGGT
Gadd45b_F	GCCCGAGACCTGCACTGCCT
Gadd45b_R	CCATTGGTTATTGCCTCTGCTCTCTT
Gadd45g_F	GGAGACCTGCATTGCATCCTCATTT
Gadd45g_R	ACTCGGGAAGGGTGATGCTGG
Apobec1_F	TCAGGGACCTTATTAGCAGCGG
Apobec1_R	GCCAATAAGCTTCGTTTGAAGGG
Apobec2_F	GACAATGGTGGCAGGCGATTCA
Apobec2_R	GCAGAGATGCTTGACTCGTTGG
Apobec3_F	TGCTACTACCACCGCATGAA
Apobec3_R	CAGCTCCATGGACCGAATCT
AID_F	GCCACCTTCGCAACAAGTCT
AID_R	CCGGGCACAGTCATAGCAC
DNMT1_F	GAGGCGGAAATCAAAGGAGGA
DNMT_R	GGGAGTCTCTGGAGCTACCT
DNMT3a_F	GGCCGAATTGTGTCTTGGTG
DNMT3a_R	CCATCTCCGAACCACATGAC
DNMT3b_F	CTGTCCGAACCCGACATAGC
DNMT3bb_R	CCGGAAACTCCACAGGGTA

qPCR primers for analysis of regeneration associated genes

Smad1_F	ACTGGCGCAGTCTGTGAAC
Smad1_R	GGTATTCGGCTCCCCAAC
Stat3_F	CTGAGCCCTCAGCAGGAG
Stat3_R	AGGTAGCACACTCCGAGGTC
EGR1_F	GAGCGAACAACCCTATGAGC
EGR1_R	AGGCCACTGACTAGGCTGAA
ATF3_F	AATTGCTGCTGCCAAGTGTC
ATF3_R	CTTCAGCTCAGCATTCACACTC

TABLE 2: Primers for enzyme-based methylation Q-PCR

ATF3_DE1_F	ACAACGAGAAGCCAGCATAG
ATF3_DE1_R	AAGGTACCATCCCCAGTCAG
ATF3_DE2_F	GTCCTTCCCTGTTGATCCAG
ATF3_DE2_R	GAAAGAGAGCCCAGATCCAG
ATF3_DE3_F	TCTGCATTGGCTCCTTACAC
ATF3_DE3_R	TGACTCAGGTGGAACACTGG
ATF3_DE4_F	TGGTTGTACCCTGTCCTTCC
ATF3_DE4_R	TGGAGAAGTTGGGGTGTCTG
ATF3_4141_F	GGCGGTGCCTTTATGACTTA
ATF3_4141_R	TGAGATGAGGTCAGGGAAGC
ATF3_PE1_F	TTGCCACTGTTATCCAGCAC
ATF3_PE1_R	AGTGACAGCTGCAACAGGAG
ATF3_PE2_F	GTCAAGACCCCTGCACAGAC
ATF3_PE2_R	CGATCCCTTCCACATTCCTC
ATF3_PE3-4_F	TCCTTTGGTACATGCCTCAG
ATF3_PE3-4_R	GTTCTGGGGTTTTTCTCCAG
ATF3_GB6_F	CTAGAATCCCAGCAGCCAAG
ATF3_GB6_R	GGCCAGCTAGGTCATCTGAG
ATF3_GB7_F	CAGAGCCTGGTGTTGTGCTA
ATF3_GB7_R	GGTGTCGTCCATCCTCTGTT
ATF3_1530_F	CTGCCTTGGACTTGAGGAAC
ATF3_1530_R	TACGGTCCTGAGGAAAGGTC
ATF3_1423_F	CTTGATTTTGCCCGAAATGT
ATF3_1423_R	GCTGCCTCCATAGCACCTAC
ATF3_1143_F	CAGACCCTCGGAATTACTGG
ATF3_1143_R	CACCGAGCCCTCTTGTACTC
Myc_dCG2_F	TGTGGCTTTCCTGTCCTTTT
Myc_dCG2_R	TAGCGGAATAGCCTGTGGTT
Myc_dCG3_F	GCTGGTGGCTACAAAGGAGA
Myc_dCG3_R	CCAAGAACCTACATTGCCTGT

TABLE 3: Primers for bisulfite sequencing

ATF3 BS_DE1_F	GATTAATAGGGAAGGATTAGGGTAAG
ATF3 BS_DE1_R	AAACCAACCTAAATAAATTCCAAAC
ATF3 BS_DE2_F	CCTAAAATACAAAAACCTAAATCAAC
ATF3 BS_DE2_R	GTTTATTAGAAAGTGGGATAGTATAAGTG
NPY BS_F	AGGAAGGTTTTATTAGTAGA
NPY BS_R	AAA AAAACCTACAACCTCCA
GAP43_BS_F	GTGTGTAGTTAGGTTATATA
GAP43_BS_R	CTCATAAATATTTAAACACCTCC
Myc_BS_F	GATGTTATTAGGTTGGGGTATAGT
Myc_BS_R	ACAATAAATAAAACTAACCCTCAAAAAATC

TABLE 4: Primers for ChIP-qPCR

GAP43_CHIP_F	TGAACCTCCATGATTATCAACTG
GAP43_CHIP_R	CTTTCCCAGTACCACAAGAAGG
ATF3_CHIP_DE1_F	ACAACGAGAAGCCAGCATAG
ATF3_CHIP_DE1_R	AAGGTACCATCCCCAGTCAG
ATF3_CHIP_DE2_F	GTCCTTCCCTGTTGATCCAG
ATF3_CHIP_DE2_R	GAAAGAGAGCCCAGATCCAG
ATF3_CHIP_DE3_F	TCTGCATTGGCTCCTTACAC
ATF3_CHIP_DE3_R	TGACTCAGGTGGAACACTGG
Myc_CHIP_dCG2_F	TGTGGCTTTCCTGTCCTTTT
Myc_CHIP_dCG2_R	TAGCGGAATAGCCTGTGGTT

LICENSE AGREEMENT

Figures etc. reprinted with permission

Licensed Content Publisher: Elsevier

Licensed Content Publication: Neuron

Licensed Content Title: “An Intrinsic Epigenetic Barrier for Functional Axon Regeneration

License Number: 4178291491756

License Date: Aug 29, 2017

BIBLIOGRAPHY

1. J. G, G., *Degeneration and Regeneration of the Nervous System.* J Neurol Psychopathol, 1929. **9**(36): p. 378-9.
2. LaFerla, F.M., K.N. Green, and S. Oddo, *Intracellular amyloid-beta in Alzheimer's disease.* Nat Rev Neurosci, 2007. **8**(7): p. 499-509.
3. Vargas, M.E. and B.A. Barres, *Why is Wallerian degeneration in the CNS so slow?* Annu Rev Neurosci, 2007. **30**: p. 153-79.
4. Beirowski, B., et al., *The progressive nature of Wallerian degeneration in wild-type and slow Wallerian degeneration (WldS) nerves.* BMC Neurosci, 2005. **6**: p. 6.
5. Griffin, J.W., et al., *Macrophage responses and myelin clearance during Wallerian degeneration: relevance to immune-mediated demyelination.* Journal of Neuroimmunology, 1992. **40**(2): p. 153-165.
6. He, Z. and V. Koprivica, *The Nogo signaling pathway for regeneration block.* Annu Rev Neurosci, 2004. **27**: p. 341-68.
7. Caroni, P. and M.E. Schwab, *Two membrane protein fractions from rat central myelin with inhibitory properties for neurite growth and fibroblast spreading.* J Cell Biol, 1988. **106**(4): p. 1281-8.
8. Schwab, M.E. and P. Caroni, *Oligodendrocytes and CNS myelin are nonpermissive substrates for neurite growth and fibroblast spreading in vitro.* J Neurosci, 1988. **8**(7): p. 2381-93.

9. Chen, M.S., et al., *Nogo-A is a myelin-associated neurite outgrowth inhibitor and an antigen for monoclonal antibody IN-1.* Nature, 2000. **403**(6768): p. 434-9.

10. GrandPre, T., et al., *Identification of the Nogo inhibitor of axon regeneration as a Reticulon protein.* Nature, 2000. **403**(6768): p. 439-44.

11. Mukhopadhyay, G., et al., *A novel role for myelin-associated glycoprotein as an inhibitor of axonal regeneration.* Neuron, 1994. **13**(3): p. 757-67.

12. Bahr, M. and C. Przyrembel, *Myelin from peripheral and central nervous system is a nonpermissive substrate for retinal ganglion cell axons.* Exp Neurol, 1995. **134**(1): p. 87-93.

13. Nathaniel, E.J. and D.C. Pease, *REGENERATIVE CHANGES IN RAT DORSAL ROOTS FOLLOWING WALERIAN DEGENERATION.* J Ultrastruct Res, 1963. **52**: p. 533-49.

14. George, R. and J.W. Griffin, *Delayed macrophage responses and myelin clearance during Wallerian degeneration in the central nervous system: the dorsal radiculotomy model.* Exp Neurol, 1994. **129**(2): p. 225-36.

15. Faulkner, J.R., et al., *Reactive astrocytes protect tissue and preserve function after spinal cord injury.* J Neurosci, 2004. **24**(9): p. 2143-55.

16. Rudge, J.S. and J. Silver, *Inhibition of neurite outgrowth on astroglial scars in vitro.* J Neurosci, 1990. **10**(11): p. 3594-603.

17. Turner, J.E. and M. Singer, *The ultrastructure of Wallerian degeneration in the severed optic nerve of the newt (Triturus viridescens).* Anat Rec, 1975. **181**(2): p. 267-85.

18. Bandtlow, C., T. Zachleder, and M.E. Schwab, *Oligodendrocytes arrest neurite growth by contact inhibition.* J Neurosci, 1990. **10**(12): p. 3837-48.

19. Aguayo, A.J., S. David, and G.M. Bray, *Influences of the glial environment on the elongation of axons after injury: transplantation studies in adult rodents.* J Exp Biol, 1981. **95**: p. 231-40.

20. David, S. and A.J. Aguayo, *Axonal elongation into peripheral nervous system "bridges" after central nervous system injury in adult rats.* Science, 1981. **214**(4523): p. 931-3.

21. Richardson, P.M., V.M. Issa, and A.J. Aguayo, *Regeneration of long spinal axons in the rat.* J Neurocytol, 1984. **13**(1): p. 165-82.

22. Blakemore, W.F., *Remyelination of CNS axons by Schwann cells transplanted from the sciatic nerve.* Nature, 1977. **266**(5597): p. 68-9.

23. Kromer, L.F. and C.J. Cornbrooks, *Transplants of Schwann cell cultures promote axonal regeneration in the adult mammalian brain.* Proc Natl Acad Sci U S A, 1985. **82**(18): p. 6330-4.

24. Kreutzberg, G.W., *Acute Neural Reaction to Injury*, in *Repair and Regeneration of the Nervous System: Report of the Dahlem Workshop on Repair and Regeneration of the Nervous Sytem Berlin 1981, November 29 – December 4*, J.G. Nicholls, Editor. 1982, Springer Berlin Heidelberg: Berlin, Heidelberg. p. 57-69.

25. Lieberman, A.R., *The Axon Reaction: A Review of the Principal Features of Perikaryal Responses to Axon Injury.* International Review of Neurobiology, 1971. **14**: p. 49-124.

26. Rossi, F., A. Jankovski, and C. Sotelo, *Differential regenerative response of Purkinje cell and inferior olivary axons confronted with embryonic grafts: environmental cues versus intrinsic neuronal determinants.* J Comp Neurol, 1995. **359**(4): p. 663-77.

27. Ziv, N.E. and M.E. Spira, *Axotomy induces a transient and localized elevation of the free intracellular calcium concentration to the millimolar range.* J Neurophysiol, 1995. **74**(6): p. 2625-37.

28. Katz, L.C. and C.J. Shatz, *Synaptic activity and the construction of cortical circuits.* Science, 1996. **274**(5290): p. 1133-8.

29. Mandolesi, G., et al., *Acute physiological response of mammalian central neurons to axotomy: ionic regulation and electrical activity.* Faseb j, 2004. **18**(15): p. 1934-6.

30. Wolf, J.A., et al., *Traumatic axonal injury induces calcium influx modulated by tetrodotoxin-sensitive sodium channels.* J Neurosci, 2001. **21**(6): p. 1923-30.

31. Pan, Y.A., et al., *Effects of neurotoxic and neuroprotective agents on peripheral nerve regeneration assayed by time-lapse imaging in vivo.* J Neurosci, 2003. **23**(36): p. 11479-88.

32. Erturk, A., et al., *Disorganized microtubules underlie the formation of retraction bulbs and the failure of axonal regeneration.* J Neurosci, 2007. **27**(34): p. 9169-80.

33. Hill, C.E., M.S. Beattie, and J.C. Bresnahan, *Degeneration and sprouting of identified descending supraspinal axons after contusive spinal cord injury in the rat.* Exp Neurol, 2001. **171**(1): p. 153-69.

34. Smith, D.S. and J.H. Skene, *A transcription-dependent switch controls competence of adult neurons for distinct modes of axon growth.* J Neurosci, 1997. **17**(2): p. 646-58.

35. Skene, J.H. and M. Willard, *Characteristics of growth-associated polypeptides in regenerating toad retinal ganglion cell axons.* J Neurosci, 1981. **1**(4): p. 419-26.

36. Chandran, V., et al., *A Systems-Level Analysis of the Peripheral Nerve Intrinsic Axonal Growth Program.* Neuron, 2016. **89**(5): p. 956-70.

37. Bareyre, F.M., et al., *In vivo imaging reveals a phase-specific role of STAT3 during central and peripheral nervous system axon regeneration.* Proc Natl Acad Sci U S A, 2011. **108**(15): p. 6282-7.

38. Seijffers, R., C.D. Mills, and C.J. Woolf, *ATF3 increases the intrinsic growth state of DRG neurons to enhance peripheral nerve regeneration.* J Neurosci, 2007. **27**(30): p. 7911-20.

39. Bomze, H.M., et al., *Spinal axon regeneration evoked by replacing two growth cone proteins in adult neurons.* Nat Neurosci, 2001. **4**(1): p. 38-43.

40. Moore, D.L., et al., *KLF Family Members Regulate Intrinsic Axon Regeneration Ability.* Science (New York, N.Y.), 2009. **326**(5950): p. 298-301.

41. Liu, K., et al., *Neuronal intrinsic mechanisms of axon regeneration.* Annu Rev Neurosci, 2011. **34**: p. 131-52.

42. Tedeschi, A. and F. Bradke, *Spatial and temporal arrangement of neuronal intrinsic and extrinsic mechanisms controlling axon regeneration.* Curr Opin Neurobiol, 2017. **42**: p. 118-127.

43. Hammarlund, M. and Y. Jin, *Axon regeneration in C. elegans.* Curr Opin Neurobiol, 2014. **27**: p. 199-207.

44. Suzuki, M.M. and A. Bird, *DNA methylation landscapes: provocative insights from epigenomics.* Nat Rev Genet, 2008. **9**(6): p. 465-76.

45. Bednar, J., et al., *Nucleosomes, linker DNA, and linker histone form a unique structural motif that directs the higher-order folding and compaction of chromatin.* Proc Natl Acad Sci U S A, 1998. **95**(24): p. 14173-8.

46. Bradbury, E.M., *K. E. Van Holde. Chromatin. Series in molecular biology. Springer-Verlag, New York. 1988. 530 pp. $98.00.* Journal of Molecular Recognition, 1989. **2**(3): p. i-i.

47. Strahl, B.D. and C.D. Allis, *The language of covalent histone modifications.* Nature, 2000. **403**(6765): p. 41-5.

48. Jenuwein, T. and C.D. Allis, *Translating the histone code.* Science, 2001. **293**(5532): p. 1074-80.

49. Spruijt, C.G. and M. Vermeulen, *DNA methylation: old dog, new tricks[quest].* Nat Struct Mol Biol, 2014. **21**(11): p. 949-954.

50. Guo, J.U., et al., *Distribution, recognition and regulation of non-CpG methylation in the adult mammalian brain.* Nat Neurosci, 2014. **17**(2): p. 215-22.

51. Feliciano, D.M., A. Bordey, and L. Bonfanti, *Noncanonical Sites of Adult Neurogenesis in the Mammalian Brain.* Cold Spring Harb Perspect Biol, 2015. **7**(10): p. a018846.

52. Cedar, H. and Y. Bergman, *Linking DNA methylation and histone modification: patterns and paradigms.* Nat Rev Genet, 2009. **10**(5): p. 295-304.

53. Fahrner, J.A. and H.T. Bjornsson, *Mendelian Disorders of the Epigenetic Machinery: Tipping the Balance of Chromatin States.* Annu Rev Genomics Hum Genet, 2014. **15**: p. 269-93.

54. Schwartz, Y.B. and V. Pirrotta, *Polycomb silencing mechanisms and the management of genomic programmes.* Nat Rev Genet, 2007. **8**(1): p. 9-22.

55. Schuettengruber, B., et al., *Trithorax group proteins: switching genes on and keeping them active.* Nat Rev Mol Cell Biol, 2011. **12**(12): p. 799-814.

56. Okano, M., S. Xie, and E. Li, *Cloning and characterization of a family of novel mammalian DNA (cytosine-5) methyltransferases.* Nat Genet, 1998. **19**(3): p. 219-20.

57. Ito, S., et al., *Role of Tet proteins in 5mC to 5hmC conversion, ES-cell self-renewal and inner cell mass specification.* Nature, 2010. **466**(7310): p. 1129-33.

58. Jeltsch, A., *Reading and writing DNA methylation.* Nat Struct Mol Biol, 2008. **15**(10): p. 1003-1004.

59. Wu, H. and Y.E. Sun, *Epigenetic regulation of stem cell differentiation.* Pediatr Res, 2006. **59**(4 Pt 2): p. 21r-5r.

60. Reik, W., *Stability and flexibility of epigenetic gene regulation in mammalian development.* Nature, 2007. **447**(7143): p. 425-32.

61. Holliday, R. and J.E. Pugh, *DNA modification mechanisms and gene activity during development.* Science, 1975. **187**(4173): p. 226-32.

62. He, Y.F., et al., *Tet-mediated formation of 5-carboxylcytosine and its excision by TDG in mammalian DNA.* Science, 2011. **333**(6047): p. 1303-7.

63. Shi, Y., et al., *Histone demethylation mediated by the nuclear amine oxidase homolog LSD1.* Cell, 2004. **119**(7): p. 941-53.

64. Plath, K., et al., *Role of histone H3 lysine 27 methylation in X inactivation.* Science, 2003. **300**(5616): p. 131-5.

65. Guo, J.U., et al., *Emerging roles of TET proteins and 5-hydroxymethylcytosines in active DNA demethylation and beyond.* Cell Cycle, 2011. **10**(16): p. 2662-8.

66. Sweatt, J.D., *The emerging field of neuroepigenetics.* Neuron, 2013. **80**(3): p. 624-32.

67. Szulwach, K.E., et al., *5-hmC-mediated epigenetic dynamics during postnatal neurodevelopment and aging.* Nat Neurosci, 2011. **14**(12): p. 1607-16.

68. Spruijt, C.G., et al., *Dynamic readers for 5-(hydroxy)methylcytosine and its oxidized derivatives.* Cell, 2013. **152**(5): p. 1146-59.

69. Trakhtenberg, E.F. and J.L. Goldberg, *Epigenetic regulation of axon and dendrite growth.* Front Mol Neurosci, 2012. **5**: p. 24.

70. Goldberg, J.L., et al., *Amacrine-signaled loss of intrinsic axon growth ability by retinal ganglion cells.* Science, 2002. **296**(5574): p. 1860-4.

71. Okano, M., et al., *DNA methyltransferases Dnmt3a and Dnmt3b are essential for de novo methylation and mammalian development.* Cell, 1999. **99**(3): p. 247-57.

72. Li, E., T.H. Bestor, and R. Jaenisch, *Targeted mutation of the DNA methyltransferase gene results in embryonic lethality.* Cell, 1992. **69**(6): p. 915-26.

73. Wu, H., et al., *Dnmt3a-dependent nonpromoter DNA methylation facilitates transcription of neurogenic genes.* Science, 2010. **329**(5990): p. 444-8.

74. Ma, D.K., et al., *Neuronal activity-induced Gadd45b promotes epigenetic DNA demethylation and adult neurogenesis.* Science, 2009. **323**(5917): p. 1074-7.

75. Lattal, K.M. and M.A. Wood, *Epigenetics and persistent memory: implications for reconsolidation and silent extinction beyond the zero.* Nat Neurosci, 2013. **16**(2): p. 124-9.

76. Su, Y., et al., *Neuronal activity modifies the chromatin accessibility landscape in the adult brain.* Nat Neurosci, 2017. **20**(3): p. 476-83.

77. Gaub, P., et al., *The histone acetyltransferase p300 promotes intrinsic axonal regeneration.* Brain, 2011. **134**(Pt 7): p. 2134-48.

78. Cho, Y., et al., *Injury-induced HDAC5 nuclear export is essential for axon regeneration.* Cell, 2013. **155**(4): p. 894-908.

79. Finelli, M.J., J.K. Wong, and H. Zou, *Epigenetic Regulation of Sensory Axon Regeneration after Spinal Cord Injury.* J Neurosci, 2013. **33**(50): p. 19664-76.

80. Kass, S.U., N. Landsberger, and A.P. Wolffe, *DNA methylation directs a time-dependent repression of transcription initiation.* Curr Biol, 1997. **7**(3): p. 157-65.

81. Kandel, E.R., J.H. Schwartz, and T.M. Jessell, *Principles of neural science*. 4th ed. ed. 2000, New York: McGraw-Hill, Health Professions Division.

82. Bauder, A.R. and T.A. Ferguson, *Reproducible mouse sciatic nerve crush and subsequent assessment of regeneration by whole mount muscle analysis.* J Vis Exp, 2012(60).

83. Bhutani, N., D.M. Burns, and H.M. Blau, *DNA Demethylation Dynamics.* Cell, 2011. **146**(6): p. 866-72.

84. Kohli, R.M. and Y. Zhang, *TET enzymes, TDG and the dynamics of DNA demethylation.* Nature, 2013. **502**(7472): p. 472-9.

85. Befort, K., et al., *Selective up-regulation of the growth arrest DNA damage-inducible gene Gadd45 alpha in sensory and motor neurons after peripheral nerve injury.* Eur J Neurosci, 2003. **18**(4): p. 911-22.

86. Kim, Y.S., et al., *Coupled Activation of Primary Sensory Neurons Contributes to Chronic Pain.* Neuron, 2016. **91**(5): p. 1085-96.

87. Rishal, I. and M. Fainzilber, *Axon-soma communication in neuronal injury.* Nat Rev Neurosci, 2014. **15**(1): p. 32-42.

88. Yu, H., et al., *Tet3 regulates synaptic transmission and homeostatic plasticity via DNA oxidation and repair.* Nat Neurosci, 2015. **18**(6): p. 836-43.

89. Costigan, M., et al., *Replicate high-density rat genome oligonucleotide microarrays reveal hundreds of regulated genes in the dorsal root ganglion after peripheral nerve injury.* BMC Neurosci, 2002. **3**: p. 16.

90. Moore, D.L. and J.L. Goldberg, *Multiple transcription factor families regulate axon growth and regeneration.* Dev Neurobiol, 2011. **71**(12): p. 1186-211.

91. Fagoe, N.D., et al., *Overexpression of ATF3 or the combination of ATF3, c-Jun, STAT3 and Smad1 promotes regeneration of the central axon branch of sensory neurons but without synergistic effects.* Hum Mol Genet, 2015. **24**(23): p. 6788-800.

92. Thakur, M., et al., *Defining the nociceptor transcriptome.* Front Mol Neurosci, 2014. **7**: p. 87.

93. Delree, P., et al., *Purification and culture of adult rat dorsal root ganglia neurons.* J Neurosci Res, 1989. **23**(2): p. 198-206.

94. Waalwijk, C. and R.A. Flavell, *MspI, an isoschizomer of hpaII which cleaves both unmethylated and methylated hpaII sites.* Nucleic Acids Res, 1978. **5**(9): p. 3231-6.

95. Jones, P.A., *Functions of DNA methylation: islands, start sites, gene bodies and beyond.* Nat Rev Genet, 2012. **13**(7): p. 484-492.

96. Belin, S., et al., *Injury-induced decline of intrinsic regenerative ability revealed by quantitative proteomics.* Neuron, 2015. **86**(4): p. 1000-14.

97. Frommer, M., et al., *A genomic sequencing protocol that yields a positive display of 5-methylcytosine residues in individual DNA strands.* Proc Natl Acad Sci U S A, 1992. **89**(5): p. 1827-31.

98. Jin, S.G., et al., *Tet3 Reads 5-Carboxylcytosine through Its CXXC Domain and Is a Potential Guardian against Neurodegeneration.* Cell Rep, 2016. **14**(3): p. 493-505.

99. Shin, J.E., S. Geisler, and A. DiAntonio, *Dynamic regulation of SCG10 in regenerating axons after injury.* Exp Neurol, 2014. **252**: p. 1-11.

100. Di Maio, A., et al., *In vivo imaging of dorsal root regeneration: rapid immobilization and presynaptic differentiation at the CNS/PNS border.* J Neurosci, 2011. **31**(12): p. 4569-82.

101. Vogelaar, C.F., et al., *Sciatic nerve regeneration in mice and rats: recovery of sensory innervation is followed by a slowly retreating neuropathic pain-like syndrome.* Brain Res, 2004. **1027**(1-2): p. 67-72.

102. Wright, M.C., et al., *Novel Roles for Osteopontin and Clusterin in Peripheral Motor and Sensory Axon Regeneration.* J Neurosci, 2014. **34**(5): p. 1689-700.

103. Chen, Q., et al., *TET2 promotes histone O-GlcNAcylation during gene transcription.* Nature, 2013. **493**(7433): p. 561-4.

104. Williams, K., et al., *TET1 and hydroxymethylcytosine in transcription and DNA methylation fidelity.* Nature, 2011. **473**(7347): p. 343-8.

105. Xue, S., et al., *TET3 Inhibits Type I IFN Production Independent of DNA Demethylation.* Cell Rep, 2016. **16**(4): p. 1096-105.

106. Mellen, M., et al., *MeCP2 binds to 5hmC enriched within active genes and accessible chromatin in the nervous system.* Cell, 2012. **151**(7): p. 1417-30.

107. Iurlaro, M., et al., *A screen for hydroxymethylcytosine and formylcytosine binding proteins suggests functions in transcription and chromatin regulation.* Genome Biol, 2013. **14**(10): p. R119.

108. Maiti, A. and A.C. Drohat, *Thymine DNA glycosylase can rapidly excise 5-formylcytosine and 5-carboxylcytosine: potential implications for active demethylation of CpG sites.* J Biol Chem, 2011. **286**(41): p. 35334-8.

109. Song, C.X., et al., *Genome-wide profiling of 5-formylcytosine reveals its roles in epigenetic priming.* Cell, 2013. **153**(3): p. 678-91.

110. Kellinger, M.W., et al., *5-formylcytosine and 5-carboxylcytosine reduce the rate and substrate specificity of RNA polymerase II transcription.* Nat Struct Mol Biol, 2012. **19**(8): p. 831-3.

111. Park, K.K., et al., *Promoting axon regeneration in the adult CNS by modulation of the PTEN/mTOR pathway.* Science, 2008. **322**(5903): p. 963-6.

112. Snider, W.D., et al., *Signaling the Pathway to Regeneration.* Neuron, 2002. **35**(1): p. 13-16.

113. Tedeschi, A., *Tuning the Orchestra: Transcriptional Pathways Controlling Axon Regeneration.* Front Mol Neurosci, 2011. **4**.

114. Smith, P.D., et al., *SOCS3 deletion promotes optic nerve regeneration in vivo.* Neuron, 2009. **64**(5): p. 617-623.

115. Sun, F., et al., *Sustained axon regeneration induced by co-deletion of PTEN and SOCS3.* Nature, 2011. **480**(7377): p. 372-375.

116. Di Cristofano, A., et al., *Pten is essential for embryonic development and tumour suppression.* Nat Genet, 1998. **19**(4): p. 348-55.

117. Suzuki, A., et al., *High cancer susceptibility and embryonic lethality associated with mutation of the PTEN tumor suppressor gene in mice.* Curr Biol, 1998. **8**(21): p. 1169-78.

118. Chen, W., et al., *Rapamycin-Resistant mTOR Activity Is Required for Sensory Axon Regeneration Induced by a Conditioning Lesion.* eNeuro, 2016. **3**(6): p. ENEURO.0358-16.2016.

119. Abe, N., et al., *Mammalian target of rapamycin (mTOR) activation increases axonal growth capacity of injured peripheral nerves.* J Biol Chem, 2010. **285**(36): p. 28034-43.

120. Gingras, A.C., B. Raught, and N. Sonenberg, *Regulation of translation initiation by FRAP/mTOR.* Genes Dev, 2001. **15**(7): p. 807-26.

121. Li, X., X. Xiong, and C. Yi, *Epitranscriptome sequencing technologies: decoding RNA modifications.* Nat Methods, 2016. **14**(1): p. 23-31.

122. Zhao, B.S., I.A. Roundtree, and C. He, *Post-transcriptional gene regulation by mRNA modifications.* Nat Rev Mol Cell Biol, 2017. **18**(1): p. 31-42.

123. Lee, M., B. Kim, and V.N. Kim, *Emerging roles of RNA modification: m(6)A and U-tail.* Cell, 2014. **158**(5): p. 980-7.

124. Gilbert, W.V., T.A. Bell, and C. Schaening, *Messenger RNA modifications: Form, distribution, and function.* Science, 2016. **352**(6292): p. 1408-12.

125. Desrosiers, R.C., K.H. Friderici, and F.M. Rottman, *Characterization of Novikoff hepatoma mRNA methylation and heterogeneity in the methylated 5' terminus.* Biochemistry, 1975. **14**(20): p. 4367-74.

126. Wang, X., et al., *N(6)-methyladenosine Modulates Messenger RNA Translation Efficiency.* Cell, 2015. **161**(6): p. 1388-1399.

127. Christie, K.J., et al., *PTEN inhibition to facilitate intrinsic regenerative outgrowth of adult peripheral axons.* J Neurosci, 2010. **30**(27): p. 9306-15.

128. Neumann, S. and C.J. Woolf, *Regeneration of dorsal column fibers into and beyond the lesion site following adult spinal cord injury.* Neuron, 1999. **23**(1): p. 83-91.

129. Neumann, S., K. Skinner, and A.I. Basbaum, *Sustaining intrinsic growth capacity of adult neurons promotes spinal cord regeneration.* Proc Natl Acad Sci U S A, 2005. **102**(46): p. 16848-52.

130. Cai, D., et al., *Arginase I and polyamines act downstream from cyclic AMP in overcoming inhibition of axonal growth MAG and myelin in vitro.* Neuron, 2002. **35**(4): p. 711-9.

131. Cai, D., et al., *Neuronal cyclic AMP controls the developmental loss in ability of axons to regenerate.* J Neurosci, 2001. **21**(13): p. 4731-9.

132. Lu, P., et al., *Combinatorial therapy with neurotrophins and cAMP promotes axonal regeneration beyond sites of spinal cord injury.* J Neurosci, 2004. **24**(28): p. 6402-9.

133. Neumann, S., et al., *Regeneration of sensory axons within the injured spinal cord induced by intraganglionic cAMP elevation.* Neuron, 2002. **34**(6): p. 885-93.

134. Butler, S.J. and G. Tear, *Getting axons onto the right path: the role of transcription factors in axon guidance.* Development, 2007. **134**(3): p. 439-48.

135. Ming, G.L. and H. Song, *Adult neurogenesis in the mammalian brain: significant answers and significant questions.* Neuron, 2011. **70**(4): p. 687-702.

136. Song, J., et al., *Neuronal Circuitry Mechanisms Regulating Adult Mammalian Neurogenesis.* Cold Spring Harb Perspect Biol, 2016. **8**(8).

137. Duan, X., et al., *Development of neural stem cell in the adult brain.* Curr Opin Neurobiol, 2008. **18**(1): p. 108-15.

138. Ninkovic, J. and M. Gotz, *Signaling in adult neurogenesis: from stem cell niche to neuronal networks.* Curr Opin Neurobiol, 2007. **17**(3): p. 338-44.

139. Gould, E., et al., *Neurogenesis in the neocortex of adult primates.* Science, 1999. **286**(5439): p. 548-52.

140. Palmer, T.D., et al., *Fibroblast growth factor-2 activates a latent neurogenic program in neural stem cells from diverse regions of the adult CNS.* J Neurosci, 1999. **19**(19): p. 8487-97.

141. Nunes, M.C., et al., *Identification and isolation of multipotential neural progenitor cells from the subcortical white matter of the adult human brain.* Nat Med, 2003. **9**(4): p. 439-47.

142. Pestronk, A., D.B. Drachman, and J.W. Griffin, *Effects of aging on nerve sprouting and regeneration.* Exp Neurol, 1980. **70**(1): p. 65-82.

143. Vaughan, D.W., *Effects of advancing age on peripheral nerve regeneration.* J Comp Neurol, 1992. **323**(2): p. 219-37.

144. Tanaka, K. and H.D. Webster, *Myelinated fiber regeneration after crush injury is retarded in sciatic nerves of aging mice.* J Comp Neurol, 1991. **308**(2): p. 180-7.

145. Verdu, E., et al., *Influence of aging on peripheral nerve function and regeneration.* J Peripher Nerv Syst, 2000. **5**(4): p. 191-208.

146. Javed, S., et al., *Clinical and diagnostic features of small fiber damage in diabetic polyneuropathy.* Handb Clin Neurol, 2014. **126**: p. 275-90.

147. Buenrostro, J.D., et al., *Transposition of native chromatin for fast and sensitive epigenomic profiling of open chromatin, DNA-binding proteins and nucleosome position.* Nat Methods, 2013. **10**(12): p. 1213-8.

148. van Berkum, N.L., et al., *Hi-C: A Method to Study the Three-dimensional Architecture of Genomes.* J Vis Exp, 2010(39).

149. Dostie, J., et al., *Chromosome Conformation Capture Carbon Copy (5C): a massively parallel solution for mapping interactions between genomic elements.* Genome Res, 2006. **16**(10): p. 1299-309.

150. Garner, C.C., R.P. Tucker, and A. Matus, *Selective localization of messenger RNA for cytoskeletal protein MAP2 in dendrites.* Nature, 1988. **336**(6200): p. 674-7.

151. Racca, C., A. Gardiol, and A. Triller, *Dendritic and postsynaptic localizations of glycine receptor alpha subunit mRNAs.* J Neurosci, 1997. **17**(5): p. 1691-700.

152. Steward, O. and E.M. Schuman, *Compartmentalized synthesis and degradation of proteins in neurons.* Neuron, 2003. **40**(2): p. 347-59.

153. Shigeoka, T., et al., *Dynamic Axonal Translation in Developing and Mature Visual Circuits.* Cell, 2016. **166**(1): p. 181-92.

154. Guo, J.U., et al., *Hydroxylation of 5-methylcytosine by TET1 promotes active DNA demethylation in the adult brain.* Cell, 2011. **145**(3): p. 423-34.

155. Song, J., et al., *Neuronal circuitry mechanism regulating adult quiescent neural stem-cell fate decision.* Nature, 2012. **489**(7414): p. 150-4.

156. Jang, M.H., et al., *Secreted frizzled-related protein 3 regulates activity-dependent adult hippocampal neurogenesis.* Cell Stem Cell, 2013. **12**(2): p. 215-23.

157. Guo, J.U., et al., *Neuronal activity modifies the DNA methylation landscape in the adult brain.* Nat Neurosci, 2011. **14**(10): p. 1345-51.

158. Shin, J.E., et al., *Dual leucine zipper kinase is required for retrograde injury signaling and axonal regeneration.* Neuron, 2012. **74**(6): p. 1015-22.

159. Duan, X., et al., *Disrupted-In-Schizophrenia 1 regulates integration of newly generated neurons in the adult brain.* Cell, 2007. **130**(6): p. 1146-58.

160. Kozlenkov, A., et al., *Differences in DNA methylation between human neuronal and glial cells are concentrated in enhancers and non-CpG sites.* Nucleic Acids Res, 2014. **42**(1): p. 109-27.

CURRICULUM VITAE

JESSICA CASSIN
Johns Hopkins University, SOM | Miller Research Building | Jcassin1@jhmi.edu

EDUCATION

Johns Hopkins University, School of Medicine **2013 - 2017**
PhD, Human Genetics

University of Maryland, Baltimore **2011 - 2012**
M.S., Human Genetics and Epidemiology

University of Louisville **2005 - 2009**
B.A., Biological Anthropology
Concentration in Natural Science
Awarded *with high honors*

RESEARCH EXPERIENCE

Johns Hopkins School of Medicine **2013 - 2017**
PhD Student
Advisor: Hongjun Song PhD
Thesis Project: Epigenetics of axon regeneration in the central and peripheral nervous system

University of Maryland, Baltimore **2011-2012**
Master's Student
Advisor: Miriam Laufer MD, MPH
Thesis: Transmission of malaria in households in Blantyre, Malawi

University of Louisville **2008 - 2009**
Undergraduate Research
Advisor: Christopher Tillquist PhD MPH
Project: Phylogeography of Tsuga canadensis

TEACHING AND SCIENCE OUTREACH EXPERIENCE

Loyola University of Maryland **2017**
Adjunct Professor - Developmental Biology

- Full responsibility of developing and teaching curriculum for an upper level class

Adjunct Professor - Cellular and Molecular Biology

- Co-taught introductory class, and individually facilitated matching lab

Johns Hopkins University School of Medicine **2015 - 2017**

Undergraduate/High School Student Trainer

- Developed incoming student orientation and lab training protocol
- Train undergraduates and high school students in proper lab safety and protocols

Smithsonian Natural History Museum **2015 - 2016**

Visiting Scientist

- Developed genetics presentations for general public in Q?rius labs
- Facilitated activities at 'Building with Biology' national event
- Facilitated roundtable discussions concerning genetic engineering

THREAD **2016**

Student Employer

- Trained high school students from THREAD program in lab safety and protocols
- Facilitated independent research

Project Bridge **2016**

Brain Fest Facilitator

- Developed and presented an interactive display on neuroscience at Johns Hopkins inaugural Brain Fest event

STEMnet **2015**

STEM Specialist

- Develop high school science curriculum in collaboration with high school science teachers
- Participated in women in STEM events at local public schools

- Presented strategies to succeed in high school and to get into college

Johns Hopkins University School of Medicine **2015**
Teaching Assistant to Roger Reeves, PhD
- Write and develop homework and exam questions on the graduate level
- Grade exams and homework
- Lead exam review sessions and hold office hours

TEACHING TRAINING

Johns Hopkins University School of Medicine **2016 - 2017**
Preparing Future Faculty Teaching Academy
- Year-long certificate program committed to training effective future teachers

PROFESSIONAL EXPERIENCE

IBM **2006 - 2013**
Client Reporting Manager
- Data analysis and auditing; managed client relations

ABSTRACTS AND PUBLICATIONS

Yi-Lan Weng, An Ran, **Jessica Cassin**, Caroline Vissers, Tianlei Xu, Xinyuan Wang, Zheng Hao Samuel Wong, Jessica Joseph, Wei Zheng, Peng Jin, Hao Wu, Xiaoxi Zhuang, Chuan He, Hongjun Song and Guo-li Ming
"Epitranscriptomic regulation of axon regeneration via m6A-dependent protein translation" Neuron (*Submitted)*

Weng YL*, An R*, **Cassin J***, Joseph J, Mi R, Chen Wang, Zhong C, Jin SG, Pfeifer GP, Bellacosa A, Dong X, Hoke A, He Z, Song H#, and Ming GL#
***Authors contributed equally to the work** "An intrinsic epigenetic barrier for functional axon regeneration" Neuron. 2017 Apr 19;94(2):337-346.

Cassin J, Jacob CG, Thesing PC, Nyirenda OM, Masonga R, Taylor TE, Plowe CV, Laufer MK (2013)
"Malaria Transmission in Households in Blantyre, Malawi" *American Society of Tropical Medicine and Hygiene*; Poster